Received: 25 April 2024 | Revised: 4 July 2024 | Accepted: 15 July 2024

DOI: 10.1111/bph.17341

RESEARCH ARTICLE

Anti-inflammatory and remyelinating effects of fexagratinib in experimental multiple sclerosis

Fynn Gurski[1] | Kian Shirvanchi[1] | Vinothkumar Rajendran[1] | Ranjithkumar Rajendran[1] | Fevronia-Foivi Megalofonou[1] | Gregor Böttiger[1] | Christine Stadelmann[2] | Sudhanshu Bhushan[3] | Süleyman Ergün[4] | Srikanth Karnati[4] | Martin Berghoff[1]

[1]Experimental Neurology, Department of Neurology, University of Giessen, Giessen, Germany

[2]Institute of Neuropathology, University Medical Centre Göttingen, Göttingen, Germany

[3]Institute for Anatomy and Cell Biology, University of Giessen, Giessen, Germany

[4]Institute of Anatomy and Cell Biology, University of Würzburg, Würzburg, Germany

Correspondence
Martin Berghoff, Department of Neurology, Justus-Liebig-University of Giessen, Klinikstrasse 33, 35385 Giessen, Germany.
Email: martinberghoff@t-online.de

Funding information
No funding was received towards this work.

Abstract

Background and Purpose: FGF, VEGFR-2 and CSF1R signalling pathways play a key role in the pathogenesis of multiple sclerosis (MS). Selective inhibition of FGFR by infigratinib in MOG_{35-55}-induced experimental autoimmune encephalomyelitis (EAE) prevented severe first clinical episodes by 40%; inflammation and neurodegeneration were reduced, and remyelination was enhanced. Multi-kinase inhibition of FGFR1-3, CSFR and VEGFR-2 by fexagratinib (formerly known as AZD4547) may be more efficient in reducing inflammation, neurodegeneration and regeneration in the disease model.

Experimental Approach: Female C57BL/6J mice were treated with fexagratinib (6.25 or 12.5 $mg \cdot kg^{-1}$) orally or placebo over 10 days either from time of EAE induction (prevention experiment) or onset of symptoms (suppression experiment). Effects on inflammation, neurodegeneration and remyelination were assessed at the peak of the disease (Day 18/20 post immunization) and the chronic phase of EAE (Day 41/42).

Key Results: In the prevention experiment, treatment with 6.25 or 12.5 $mg \cdot kg^{-1}$ fexagratinib prevented severe first clinical episodes by 66.7% or 84.6% respectively. Mice treated with 12.5 $mg \cdot kg^{-1}$ fexagratinib hardly showed any symptoms in the chronic phase of EAE. In the suppression experiment, fexagratinib resulted in a long-lasting reduction of severe symptoms by 91 or 100%. Inflammation and demyelination were reduced, and axonal density, numbers of oligodendrocytes and their precursor cells, and remyelinated axons were increased by both experimental approaches.

Abbreviations: BBB, blood–brain barrier; EAE, experimental autoimmune encephalomyelitis; MOG, myelin oligodendrocyte glycoprotein; MS, multiple sclerosis; NAWM, normal-appearing white matter; OPCs, oligodendrocyte precursor cells; p.i., post immunization; WML, white matter lesions.

Fynn Gurski and Kian Shirvanchi contributed equally to this work.

Conclusion and Implications: Multi-kinase inhibition by fexagratinib in a well-tolerated dose of 1 $mg \cdot kg^{-1}$ in humans may be a promising approach to reduce inflammation and neurodegeneration, to slow down disease progression and support remyelination in patients.

KEYWORDS

AZD4547, demyelination, experimental autoimmune encephalomyelitis, fexagratinib, inflammation, multi-kinase inhibition, multiple sclerosis, remyelination

1 | INTRODUCTION

Multiple sclerosis (MS) is an autoimmune-mediated inflammatory and demyelinating disease of the CNS. Approximately 2.8 million people worldwide are diagnosed with MS, which predominantly affects women between the ages of 20 and 40 years (Walton et al., 2020). The underlying pathology includes migration of lymphocytes and monocytes across the blood–brain barrier (BBB), followed by destruction of oligodendrocytes, demyelination and axonal degeneration in the CNS (Charabati et al., 2023; Kunkl et al., 2020; Reich et al., 2018). In MS, remyelination is known to be impaired due to a decrease in migration and differentiation of oligodendrocyte progenitor cells (OPC) (Lassmann, 2019; Mahad et al., 2015).

Investigations of brain autopsy tissue and cerebral spinal fluid (CSF) suggest that FGF/**FGFR**, CSF/**CSFR** and **VEGF**/**VEGFR-2** signalling pathways play a role in the pathology of MS. In chronic brain lesions, **FGF-1** is expressed in oligodendrocytes, microglia/macrophages and lymphocytes (Mohan et al., 2014); **FGF-2** is mainly found in microglia/macrophages, and **FGFR1** is up-regulated in oligodendrocyte precursor cells (Clemente et al., 2011). CSFR is increased in lesions in MS and EAE (Hagan et al., 2020). Moreover, higher levels of FGF-2 and CSF1 were found in the CSF during progressive MS (Hagan et al., 2020; Sarchielli et al., 2008). Overexpression of **VEGF** was observed in reactive astrocytes in plaques and in the serum of patients during relapses (Amini Harandi et al., 2022; Proescholdt et al., 2002; Su et al., 2006).

In MOG_{35-55}-induced experimental autoimmune encephalomyelitis (EAE), oligodendrocyte specific knock-out of *FGFR1* or *FGFR2* mice resulted in a milder disease course, decreased infiltration of lymphocytes and macrophages/microglia in demyelinating lesions, and less degeneration of myelin and axons (Kamali et al., 2021; Rajendran et al., 2021). These effects in $Fgfr^{ind-/-}$ mice were accompanied by changes in **ERK**/**Akt** phosphorylation, and expression of **BDNF** and **TrkB** (Rajendran et al., 2021). ERK/Akt pathways are also activated by the VEGFR-2 and CSFR. In MBP_{68-82}-induced EAE, an increase in VEGF(+) astrocytes was detected in the acute phase of EAE (Proescholdt et al., 2002). The CSFR has been shown to mediate chemotaxis of macrophages/microglia in the cuprizone model of MS (Marzan et al., 2021). Thus, several lines of evidence indicate abnormal regulation of FGF/FGFR, CSF/CSFR and VEGF/VEGFR-2 pathways in MS and EAE, offering targets for pharmacological interventions.

Current disease modifying treatment (DMT) effectively reduces relapses and formation of lesions in the CNS by modulating peripheral immune cell responses. **Sphingosine-1-phosphate receptor** (S1P receptor) modulators such as fingolimod or ponesimod, prevent exit of lymphocytes from lymph nodes, natalizumab inhibits migration of

What is already known?

- FGF, VEGFR-2 and CSFR signalling pathways play a key role in multiple sclerosis.
- Fexagratinib is a multi-kinase inhibitor of FGFR1-3, VEGFR-2 and CSFR

What does this study add?

- Fexagratinib reduces symptom severity, inflammation, demyelination and neurodegeneration.
- Fexagratinib enhances numbers of oligodendrocytes and remyelination.

What is the clinical significance?

- Increasing oligodendrocyte numbers and remyelination is an unmet goal in MS therapy.
- Fexagratinib may be a promising approach to reduce disease progression and support remyelination in patients.

immune cells into the CNS, and anti-CD20 antibodies deplete B cells (Chisari et al., 2022; Khoy et al., 2020; Roy et al., 2021). As these substances do not cross the BBB, they do not promote remyelination in the CNS (Dendrou et al., 2015). Phase II/III studies with compounds known to induce remyelination in disease models, such as LINGO-1 inhibitor opicinumab, have failed (Cadavid et al., 2019). Thus, despite an increasing number of DMTs for patients, there is a need for specific therapeutics which act in the CNS on oligodendrocytes and promote remyelination (Derdelinckx et al., 2021; Freeman et al., 2022).

In a recent MOG_{35-55}-induced EAE study, oral administration of the selective FGFR inhibitor infigratinib prevented severe first clinical episodes by 40% (Rajendran et al. 2023). Treatment with infigratinib resulted in reduced immune cell infiltration in white matter lesions (WML). The number of oligodendrocytes was increased in WML, and remyelination was found (Rajendran et al., 2023). In other MOG_{35-55}-induced EAE experiments, CSFR and VEGFR-2 inhibitors revealed beneficial effects on the disease course, decreased immune cell infiltration and reduced demyelination (Hagan et al., 2020; Hwang et al., 2022; Roscoe et al., 2009).

Fexagratinib (formerly known as AZD4547), a pyrazoloamide derivative, offers wider inhibition of signalling pathways associated with MS pathology. Fexagratinib potently inhibits the tyrosine kinase activity of FGFR1-3, CSFR and VEGFR-2. The efficacy of fexagratinib has been demonstrated in experimental tumour models and is currently undergoing evaluation in phase II clinical tumour trials. Common side effects include fatigue, constipation, decreased appetite and hyperphosphataemia (Gavine et al., 2012; Paik et al., 2017). In the present EAE study, fexagratinib (6.25 or 12.5 $mg{\cdot}kg^{-1}$) or placebo was administered orally over 10 days, either from the time of EAE induction or the onset of symptoms. We hypothesized that multi-kinase inhibition has stronger effects on the disease course, inflammation, neurodegeneration and remyelination than selective FGFR inhibition.

2 | METHODS

2.1 | Ethics statement and experimental conditions

All scientific procedures on animals were approved by the regional council of Giessen, Hesse, Germany (GI 20/18 Nr. G38/2020) in accordance with the German Animal Welfare Act and the European legislation for the protection of animals used for scientific purposes (2010/63/EU). AVMA guidelines for animal euthanasia were followed. Animal studies are reported in compliance with the ARRIVE guidelines (Percie du Sert et al., 2020) and with the recommendations made by the *British Journal of Pharmacology* (Lilley et al., 2020).

Seven-week-old female C57BL/6 J mice (*Mus musculus*; Charles River Laboratories, Sulzfeld, Germany), were housed in a controlled environment and maintained on a 12-h light/dark cycle (Biomedical Research Centre Seltersberg, Justus-Liebig-University). The acclimation period in the animal facility lasted 1 week. Mice had free access to a standard pellet diet (Altromin 1324 TPF, Altromin Spezialfutter GmbH, Lage, Germany) and autoclaved water. Mice with limb weakness were housed in cages with cellulose bedding and food enrichment, including diet gel boost, wet food and hydrogel. Humane endpoints were an EAE-Score of 3.5 over 5 days and loss of defaecation.

2.2 | Experimental autoimmune encephalomyelitis (EAE) induction and evaluation of symptoms

Eight-week-old female C57BL/6J mice were immunized with 300 µg myelin oligodendrocyte glycoprotein peptide s.c. (MOG_{35-55}; Institute of Medical Immunology, Charité University Hospital, Berlin, Germany) emulsified in complete Freund's adjuvant (CFA) (Sigma, Steinheim, Germany) containing 10 mg heat-inactivated *Mycobacterium tuberculosis* (Difco, Plymouth, MI, USA). Pertussis toxin (300 ng; Calbiochem, Darmstadt, Germany) was administered i.p. on days 0 and 2. Mice were scored at least once a day in a blinded fashion using five-point grading criteria: 0 = *normal*, 0.5 = *distal tail weakness*, 1 = *complete tail weakness*, 1.5 = *mild hind limb weakness*, 2 = *ascending hind limb weakness*, 2.5 = *severe hind limb weakness*, 3 = *hind limb paralysis*, 3.5 = *hind limb paralysis and moderate forelimb weakness*, 4 = *hind limb paralysis and severe forelimb weakness*, 4.5 = *tetraplegia and incontinence*, 5 = *moribund/dead*. Tissues were collected on days 18 post-immunization (p.i.) and 41 p.i. (prevention experiment), and on days 20 p.i. and 42 p.i. (suppression experiment).

2.3 | Administration of fexagratinib

The multi-kinase inhibitor fexagratinib (S2801; Selleck Chemicals, Houston, TX, USA) was dissolved in 4% dimethyl sulfoxide (DMSO, Carl Roth, Karlsruhe, Germany), 30% PEG300 (AppliChem, Darmstadt, Germany), 5% TWEEN 80 (Sigma-Aldrich, St. Louis, MO, USA), and 61% ddH2O according to the manufacturer's instructions and stored at 4°C. Oral doses of fexagratinib (6.25 or 12.5 $mg{\cdot}kg^{-1}{\cdot}day^{-1}$) or 100 µl vehicle (dissolved substances without fexagratinib) were administered using a feeding tube (FTP-22-25; Linton Instrumentation, Palgrave, UK) from Day 0 to 9 p.i. (prevention experiment), or from Day 10 to 19 p.i. (suppression experiment). Fexagratinib dosages of 6.25/12.5 $mg{\cdot}kg^{-1}$ were selected based on recent pharmacokinetics/pharmacodynamics (PK/PD) studies, indicating that these doses efficiently inhibit FGFR in mouse models (Gavine et al., 2012).

2.4 | Tissue protein extraction and western blot analysis

Quantification of proteins were performed as described previously, by using spinal cord tissue (Rajendran et al., 2023). Primary antibodies for target proteins and the corresponding secondary antibodies are listed in the methods. GAPDH was used as a loading control. Images were taken by using an ECL ChemoCam Imager (INTAS Science Imaging Instruments GmbH, Göttingen, Germany). Protein band densities were analysed using ImageJ 1.53b software (National Institute of Health, Bethesda, MD, USA).

2.5 | RNA isolation, cDNA synthesis and RT-PCR

RT-PCR was used to measure the relative mRNA expression of each gene in the spinal cord as described previously (Rajendran et al., 2023). The mRNA expression of FGFR1/2, pro-inflammatory cytokines (**IL-1β**, **IL-6**, **IL-12**, **iNOS** and IFNγ), chemokines (**CX_3CL1** and **CX_3CR1**) and remyelination inhibitors (**TGFβ**, SEMA3A and LINGO-1) were measured. Target gene quantification was performed using the primer sequences listed in the methods. Target gene expression was normalized to the level of GAPDH, and the comparative ΔΔCT method was used to measure the gene expression.

2.6 | Histopathology and immunohistochemistry

For histopathological, immunohistochemical and immunohistochemistry investigations, we followed the procedure described before by using spinal cord tissue (Rajendran et al., 2023). Haematoxylin and eosin stain (H&E) was used to assess inflammatory infiltrates, Luxol fast blue/periodic acid-Schiff staining (LFB/PAS) to investigate demyelination, and Bielschowsky silver impregnation to evaluate axonal degeneration. For immunohistochemistry, primary and secondary antibodies are listed in the methods. To assess the degree of inflammatory infiltration, a semiquantitative score (inflammation index) ranging from 0 to 5 was applied as described before (Rajendran et al., 2023): 0: *no inflammation*; 1–4: *increasing number of inflammatory cells*; 5: *total cell accumulation*. Demyelination was calculated by dividing the WML area by the total white matter area (in percent). Axonal density was calculated by the mean number of axons in WML divided by the mean number of axons in NAWM (in percent). Immunohistochemical findings (CD3(+) T cells, B220(+) B cells, Mac3(+) macrophages/microglia, Olig2(+) OPC and p25(+) mature oligodendrocytes) were quantified in a minimum of five spinal cord sections per mouse in WML and NAWM and normalized to an area of 1 mm^2. Both histopathological and immunohistochemical analyses were digitalized by Axio Scan Z1 Microscope and quantified with ZEN 3.2 (blue edition) software (Carl Zeiss Microscopy GmbH, Oberkochen, Germany). The Immuno-related procedures used comply with the recommendations made by the British Journal of Pharmacology (Alexander et al., 2018).

2.7 | Ultrastructural analysis

For ultrastructural investigation of myelin sheaths and axons we followed the same protocol described recently (Rajendran et al., 2023). After preparation, tissue was analysed by a Zeiss LEO 906 transmission electron microscope (Carl Zeiss AG, Oberkochen, Germany). Images were taken with a digital camera (Tröndle sharp eye camera, Moorenweis, Germany) using Image SP Version 1.2.3.46 (Unitary Enterprise 'SYSPROG', Minsk, Belarus) at magnifications between 1000X and 2000X. Images were taken of lesions of the ventrolateral column of the lumbar parts of the spinal cord. At least five images were taken per tissue. Remyelinated axons were identified by neuropathological characteristics such as thinner myelin sheaths in relation to the axon diameter and counted using ImageJ Version 1.53 (National Institutes of Health, Bethesda, MD, USA) and normalized to an area of 1000 μm^2.

2.8 | FACS analysis

To study the response of the peripheral immune cells, flow cytometry analyses of the spleen and blood were performed as described previously (Rajendran et al., 2023). All cells were incubated with an Fc blocker (Miltenyi Biotec, Bergisch Gladbach, Germany) and with respective fluorescent-labelled antibodies (listed in methods). Macrophages, dendritic cells and granulocytes were gated on single and live cells, whereas the dead cells were excluded by DAPI staining. To identify the leucocyte populations, cell aggregates and dead cells were excluded using SSC-A versus SSC-H gating. Further gating aimed at the detection of CD19+ and CD3+ populations. Identified CD3+ cells were further stratified in CD4+ and CD8+ cell populations. All cell populations were measured in terms of proportions, since non-red-blood-cell-lysed samples were clumping and the size of each tissue varied. By comparing specific cell populations against all singular haematopoietic nucleated cells, as described by Rajendran (Rajendran et al., 2023), we achieved a robust normalization, which allowed differential comparison of cell populations of interest. Flow cytometry analysis was performed using a MACSQuant Analyzer 10 flow cytometer (Miltenyi Biotec, Bergisch Gladbach, Germany). Data were analysed with FlowJo software version X (Tree Star, Ashland, OR, USA).

2.9 | Materials

2.9.1 | Primary antibodies used for WB and IHC

Name	Host	Reactivity	Mol. weight	Method	Art. no	Manufacturer
Anti-FGF-2	Mouse	H, M, R	18, 21, 24 kDa	WB	Sc-365106	Santa Cruz Biotech, CA, USA
Anti-FGF-9	Mouse	H, M, R	30 kDa	WB	Sc-8413	Santa Cruz Biotech,
Anti-CNPase	Mouse	H, M, R	46 kDa	WB	Sc-166019	Santa Cruz Biotech,
Anti-MBP	Mouse	H, M, R, G	12,18 kDa	WB	78896S	Cell Signaling Tech, MA, USA
Anti-PLP	Rabbit	H, M, R	30 kDa	WB	85971	Cell Signaling Tech,
Anti-pERK p-44/42	Rabbit	H, M, R, Hm, Mk	44, 42 kDa	WB	4370s	Cell Signaling Tech,
Anti-pAkt (Ser473)	Rabbit	H, M, R, MK	60 kDa	WB	4060s	Cell Signaling Tech,
Anti-FGFR1	Rabbit	H, M, R	110 kDa	WB	Sc-57132	Santa Cruz Biotech,
Anti-FGFR2	Rabbit	H, M, R	120 kDa	WB	Sc-6930	Santa Cruz Biotech,
Anti-GAPDH	Mouse	H, M, R	37 kDa	WB	Sc-365062	Santa Cruz Biotech,
Anti-TrkB	Rabbit	H, M, R	145 kDa	WB	Sc-377218	Santa Cruz Biotech,
Anti-pro BDNF	Rabbit	H, M, R	14 kD	WB	Sc-65514	Santa Cruz Biotech,
Anti-VEGFR-2	Rabbit	H, M, R	210	WB	9698S	Cell Signaling Tech,
Anti-CSFR	Rabbit	M, R	108 kDa	WB	ab221684	Abcam, Cambridge, UK
Anti-ATP synthase β	Mouse	H, M, R	57 kDa	WB	A21351	Invitrogen, MA, USA
Anti-ATP6E	Mouse	H, M, R	33 kDa	WB	Sc-514,143	Santa Cruz Biotech,
Anti-SOD2	Rabbit	H, M, R, Mk	25 kDa	WB	13194S	Cell Signaling Tec
Mac 3 clone M3/84	Rat	M	Staining	IHC	553322	BD biosciences
B220 clone RA3-6B2	Rat	H, M	Staining	IHC	557390	BD biosciences
CD3, clone CD3–12	Rat	M	Staining	IHC	MCA 1477	Bio-rad labs, CA, USA
Olig2	Mouse	H, M, R	Staining	IHC	MABN50	MerckMillipore, Germany
P25	Rabbit	H, M, R	Staining	IHC	Ab 92305	Abcam

2.9.2 | Secondary antibodies used for WB

Name	Host	Method	Art. No	Manufacturer
Anti-rabbit-HRP	Goat	WB	7074	Cell Signaling Tech
Anti-mouse-HRP	Horse	WB	7076	Cell Signaling Tech

2.9.3 | Primers used for PCR

Primer	5′ → 3′ sequence
IFNγ	Forward: CGG CAC AGT CAT TGA AAG CC
	Reverse: TGC ATC CTT TTT CGC CTT GC
IL1β	Forward: TAC CTG TGG CCT TGG GCC TCA A
	Reverse: GCT TGG GAT CCA CAC TCT CCA GCT
IL6	Forward: CTC TGC AAG AGA CTT CCA
	Reverse: AGT CTC CTC TCC GGA CTT
IL12	Forward: AGA CCA CAG ATG ACA TGG TGA
	Reverse: ACG ACG TGG GCT ACA GGC TT
iNOS	Forward: TTG GAG GCC TTG TGT CAG CCC T
	Reverse: AAG GCA GCG GGC ACA TGC AA
GAPDH	Forward: TGG CAA AGT GGA GAT TGT TGC C
	Reverse: AAG ATG GTG ATG GGC TTC CCG
TGFβ	Forward: CTC CTG CTG CTT TCT CCC TC
	Reverse: GTG GGG TCT CCC AAG GAA AG
SEMA3A	Forward: GGA TGG GTC CTC ATG CTC AC
	Reverse: TGG TGC TGC AAG TCA GAG CAG
LINGO1	Forward: TCA TCA GGT GAG CGA GAG GA
	Reverse: CAG TAC CAG CAG GAG GAT GG
CX_3CR1	Forward: CTG CTC AGG ACC TCA CCA TGT
	Reverse: ATG TCG CCC AAA TAA CAG GC
CX_3CL1	Forward: CTG CTC AGG ACC TCA CCA TGT
	Reverse: ATG TCG CCC AAA TAA CAG GC

All primers were purchased from Eurofins Genomics Germany GmbH, Ebersberg, Germany.

(Continues)

2.9.4 | Antibodies used for FACS

Fluorophore	Marker	Catalogue	Clone	Dilution
Pacific blue	CD3	100214	17A2	1:50
Brilliant violet 510™	CD4	116025	RM4-4	1:80
Alexa Fluor® 488	CD8	100723	53-6.7	1:200
APC	CD19	115520	6D5	1:80
Brilliant violet 510™	GR1	108438	RB6-8C5	1:20
PerCP/Cyanine5.5	CD11b	101228	M1/70	1:80
APC/Cyanine7	CD11c	117324	N418	1:20

FACS antibodies were purchased from BioLegend Way, CA, USA

2.10 | Data and statistical analysis

Data and statistical analysis complied with the recommendations of the *British Journal of Pharmacology* on experimental design and analysis in pharmacology (Curtis et al., 2022).

All analyses were performed in a blinded fashion. EAE scores from two independent experiments were analysed using a Kruskal–Wallis test. Each group contained 13–15 mice, and 78–84 mice were used in each experiment. In total, 162 mice were used without exclusion. Calculation of the sample size was based on our previous study (Rajendran et al., 2023). For immunohistochemical analysis, positively stained cells were counted in a minimum of five spinal cord sections per mouse. Histological and immunohistochemical data were analysed by Student's *t* test. Western blot and RT-PCR data were analysed by one-way ANOVA followed by post hoc Bonferroni multiple comparison test. Post-hoc tests were run only if F achieved P<0.05 and there was no significant variance inhomogeneity. Please confirm this was done.A summary of results is shown in Supplementary Table S1. Statistical analysis and graph preparation were performed using GraphPad Prism Version 9 (GraphPad Software, San Diego, CA, USA). Statistical significance was set at $P \leq 0.05$. Data are expressed as mean ± standard error of the mean (SEM); ns = not significant.

2.11 | Nomenclature of targets and Ligand

Key protein targets and ligands in this article are hyperlinked to corresponding entries in the IUPHAR/BPS Guide to PHARMACOLOGY http://www.guidetopharmacology.org and are permanently archived in the Concise Guide to PHARMACOLOGY 2023/23 (Alexander, Christopoulos, Davenport, Kelly, Mathie, Peters, Veale, Armstrong, Faccenda, Harding, Davies, et al., 2023; Alexander, Fabbro, Kelly, Mathie, Peters, Veale, Armstrong, Faccenda, Harding, Davies, Amarosi, et al., 2023; Alexander, Fabbro, Kelly, Mathie, Peters, Veale, Armstrong, Faccenda, Harding, Davies, Annett, et al., 2023; Alexander, Fabbro, Kelly, Mathie, Peters, Veale, Armstrong, Faccenda, Harding, Davies, Beuve, et al., 2023).

3 | RESULTS

3.1 | Treatment with fexagratinib reduces symptoms of experimental autoimmune encephalomyelitis (EAE)

To study the effects of fexagratinib on the disease course, mice were administered fexagratinib (6.25 or 12 $mg \cdot kg^{-1}$) or placebo from Day 0 to 9 p.i. (prevention experiment) or from Day 10 to 19 p.i. (suppression experiment) (Figure 1a).

In the prevention experiment, application of fexagratinib at a dose of 6.25 or 12.5 $mg \cdot kg^{-1}$ did not affect the onset of symptoms (Figure 1g). At the peak of the disease (Day 18 p.i.), the mean EAE scores were 0.71 ± 0.19 (6.25 $mg \cdot kg^{-1}$), 0.33 ± 0.10 (12.5 $mg \cdot kg^{-1}$) or 2.13 ± 0.16 (placebo) ($P < 0.05$; Figure 1f). At Day 18 p.i., 50% of mice on placebo were severely affected (EAE scores ≥2.5), compared with 4% of mice treated with 6.25 $mg \cdot kg^{-1}$ of fexagratinib ($P < 0.05$; Figure 1b). None of the mice on 12.5 $mg \cdot kg^{-1}$ of fexagratinib were severely affected ($P < 0.05$; Figure 1b). At Day 41 p.i., none of the mice treated with 12.5 $mg \cdot kg^{-1}$ of fexagratinib were severely affected compared to 8% on 6.25 $mg \cdot kg^{-1}$ of fexagratinib or 45% on placebo ($P < 0.05$ and $P = 0.409$; Figure 1c).

Only on Day 18 p.i., body weight of mice on placebo was lower than of mice on fexagratinib (Figure 1h).

In the suppression experiment, application of fexagratinib resulted in mean EAE scores of 0.71 ± 0.15 (6.25 $mg \cdot kg^{-1}$), 0.39 ± 0.11 (12.5 $mg \cdot kg^{-1}$) or 2.04 ± 0.17 (placebo) ($P < 0.05$; Figure 1i) at Day 20 p.i. At Day 20 p.i., none of the mice on 12.5 $mg \cdot kg^{-1}$ of fexagratinib were severely affected (EAE score ≥2.5), compared to 4% of mice on 6.25 $mg \cdot kg^{-1}$ of fexagratinib ($P < 0.05$; Figure 1d) and 37% of mice on placebo ($P < 0.05$; Figure 1d). Application of 6.25 or 12.5 $mg \cdot kg^{-1}$ of AZD4574 resulted in long-lasting effects on symptoms (Figure 1i). At Day 42 p.i., none of the mice on 12.5 $mg \cdot kg^{-1}$ of fexagratinib, 8% of mice on 6.25 $mg \cdot kg^{-1}$ of fexagratinib and 33% of mice on placebo were severely affected ($P < 0.05$; Figure 1e).

No differences in body weight were observed between the groups (Figure 1k).

3.2 | Application of fexagratinib decreased inflammation, demyelination and axonal degeneration and enhanced remyelination

To investigate the effects of 12.5 $mg \cdot kg^{-1}$ of fexagratinib on inflammation, demyelination, axonal degeneration and remyelination, spinal cord tissue was analysed.

In the prevention experiment, application of fexagratinib led to reduced inflammation at Days 18 p.i. and 41 p.i. (Figure 2a,b). CD3 (+) T cells, B220(+) B cells and Mac3(+) macrophages/microglia were decreased in WML at Days 18 p.i. (Figure 2a) and 41 p.i. (Figure 2b). Further, treatment with fexagratinib resulted in less

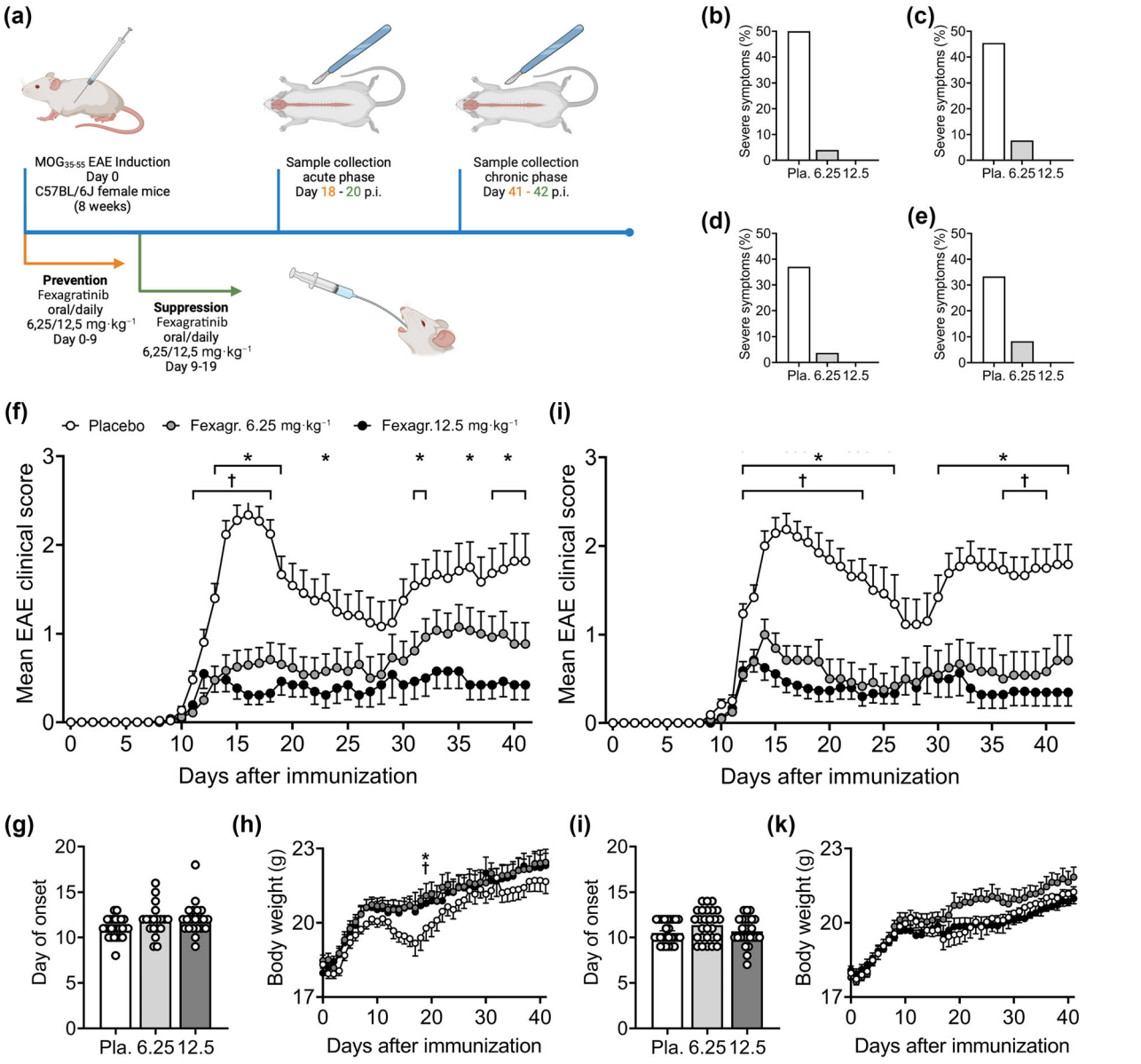

FIGURE 1 Experimental design and efficacy of fexagratinib in experimental autoimmune encephalomyelitis (EAE). (a) Experimental design: MOG_{35-55}-induced EAE, administration of fexagratinib and time points of analysis. (b–e) Mice with severe symptoms (EAE score ≥2.5). (b, c) Prevention experiment. (b) Day 18 post immunization (p.i.); (c) Day 41 p.i. (d, e) Suppression experiment. (d) Day 20 p.i.; (e) Day 42 p.i. (f) EAE disease course in mice treated with fexagratinib in the *prevention experiment* (6.25 $mg \cdot kg^{-1}$ of fexagratinib, n = 13; 12.5 $mg \cdot kg^{-1}$ of fexagratinib, n = 13) or placebo (n = 13). For detailed *P* values, see Supplementary Table 1. (g) Day at onset in the *prevention experiment*. (h) Body weight in the *prevention experiment*. (i) EAE disease course in mice treated with fexagratinib during *suppression experiment* (6.25 $mg \cdot kg^{-1}$ of fexagratinib, n = 13; 12.5 $mg \cdot kg^{-1}$ of fexagratinib, n = 13) or placebo (n = 13). For detailed *P* values, see Supplementary Table 2. (j) Day at onset in the *suppression experiment*. (k) Body weight in the *suppression experiment*. *: Placebo vs fexagratinib 12.5 $mg \cdot kg^{-1}$. †: Placebo versus fexagratinib 6.25 $mg \cdot kg^{-1}$. Data are presented as mean ± SEM. Fexagr., fexagratinib; Pla, placebo.

demyelination at Days 18 p.i. and 41 p.i. as well as increased axonal densities at Days 18 p.i. and 41 p.i. (Figure 2c,d). Ultrastructural analysis revealed a higher number of remyelinated axons in WML in mice treated with fexagratinib at Days 18 p.i. and 41 p.i. (Figure 5a–c).

In the suppression experiment, application of fexagratinib caused a reduction in inflammation at Days 20 p.i. and 42 p.i. (Figure 3a,b). CD3(+) T cells, B220(+) B cells and Mac3(+) macrophages/microglia were decreased in WML at Days 20 p.i. (Figure 3a) and 41 p.i. (Figure 3b). Fexagratinib treatment also decreased demyelination at Days 20 p.i. and 42 p.i. and increased axonal densities at Days 20 p.i. and 42 p.i. (Figure 3c,d). Additionally, application of fexagratinib led to a higher number of remyelinated axons in WML at Days 20 p.i. and 42 p.i. (Figure 6a–c).

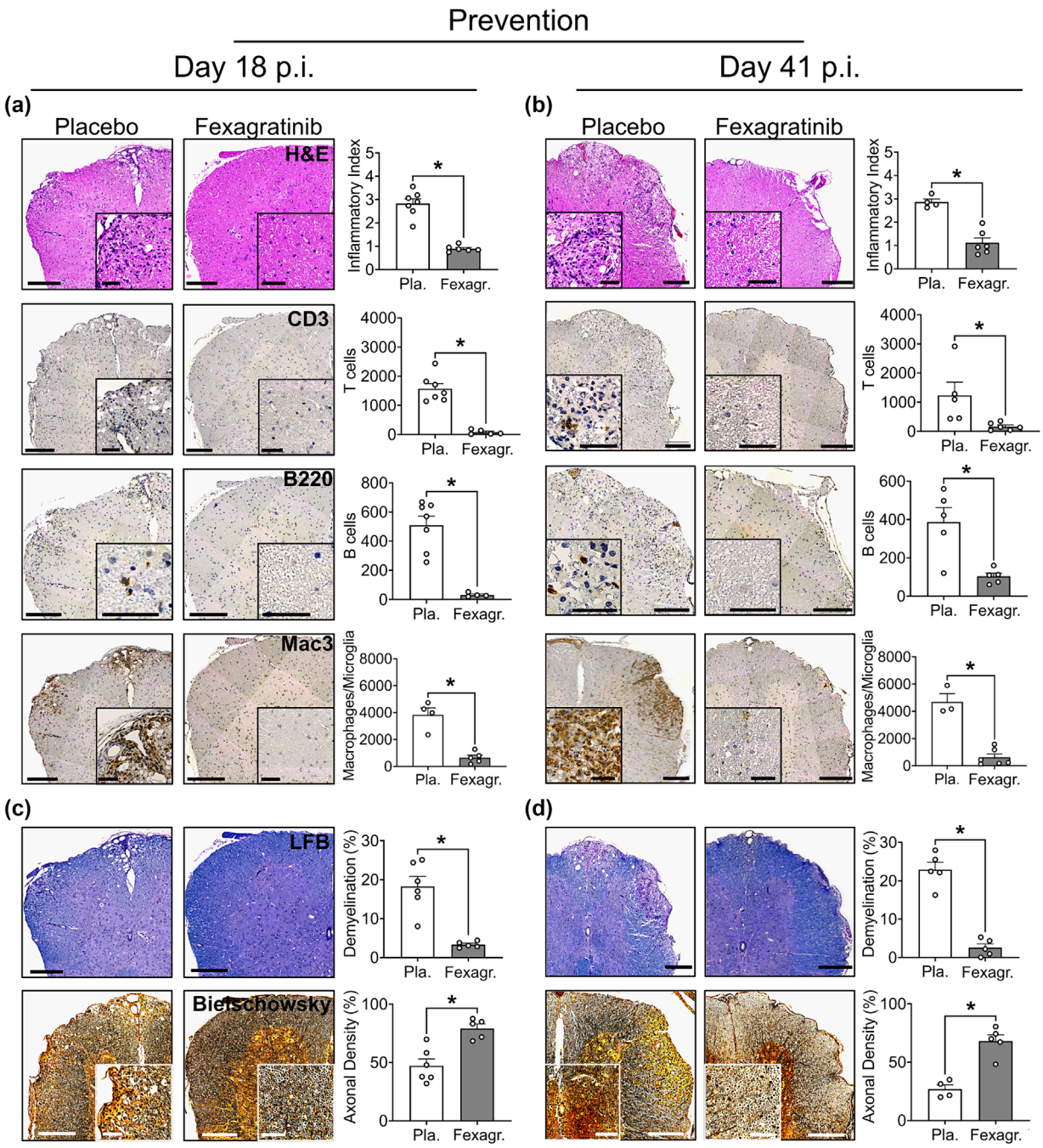

FIGURE 2 Effects of fexagratinib on inflammation and neurodegeneration in the spinal cord (prevention experiment). Inflammatory index, the number of CD3(+) T cells, B220(+) B cells and Mac3(+) macrophages/microglia in white matter lesions (WML) (a) at Day 18 post immunization (p.i.) and (b) at Day 41 p.i. Demyelination (LFB/PAS) and the number of axons (Bielschowsky staining) in WML (c) at Day 18 p.i. and (d) at Day 41 p.i. Representative images of spinal cord sections are shown. Scale bars represent 200 μm and 50 μm. n = 3–7/group. Data are presented as mean ± SEM. Fexagr., fexagratinib; Pla, placebo.

3.3 | Treatment with fexagratinib resulted in increased numbers of Olig2(+) OPCs and mature oligodendrocytes in white matter lesions (WML)

To assess the effects of 12.5 mg·kg^{-1} of fexagratinib on oligodendrocyte populations, the numbers of Olig2(+) OPCs and p25(+) mature oligodendrocytes in WML and normal appearing white matter (NAWM) were analysed. Additionally, the effects of fexagratinib (at doses of 6.25 and 12.5 mg·kg^{-1}) on myelin protein expression and levels of remyelination inhibitor mRNA were evaluated.

In the prevention experiment, fexagratinib caused an increase in the number of p25(+) mature oligodendrocytes in WML at Day 18 p.i. (Figure 4b). A trend towards an increased number of Olig2(+) OPCs was found ($P = 0.055$; Figure 4a). At Day 41 p.i., the number of Olig2

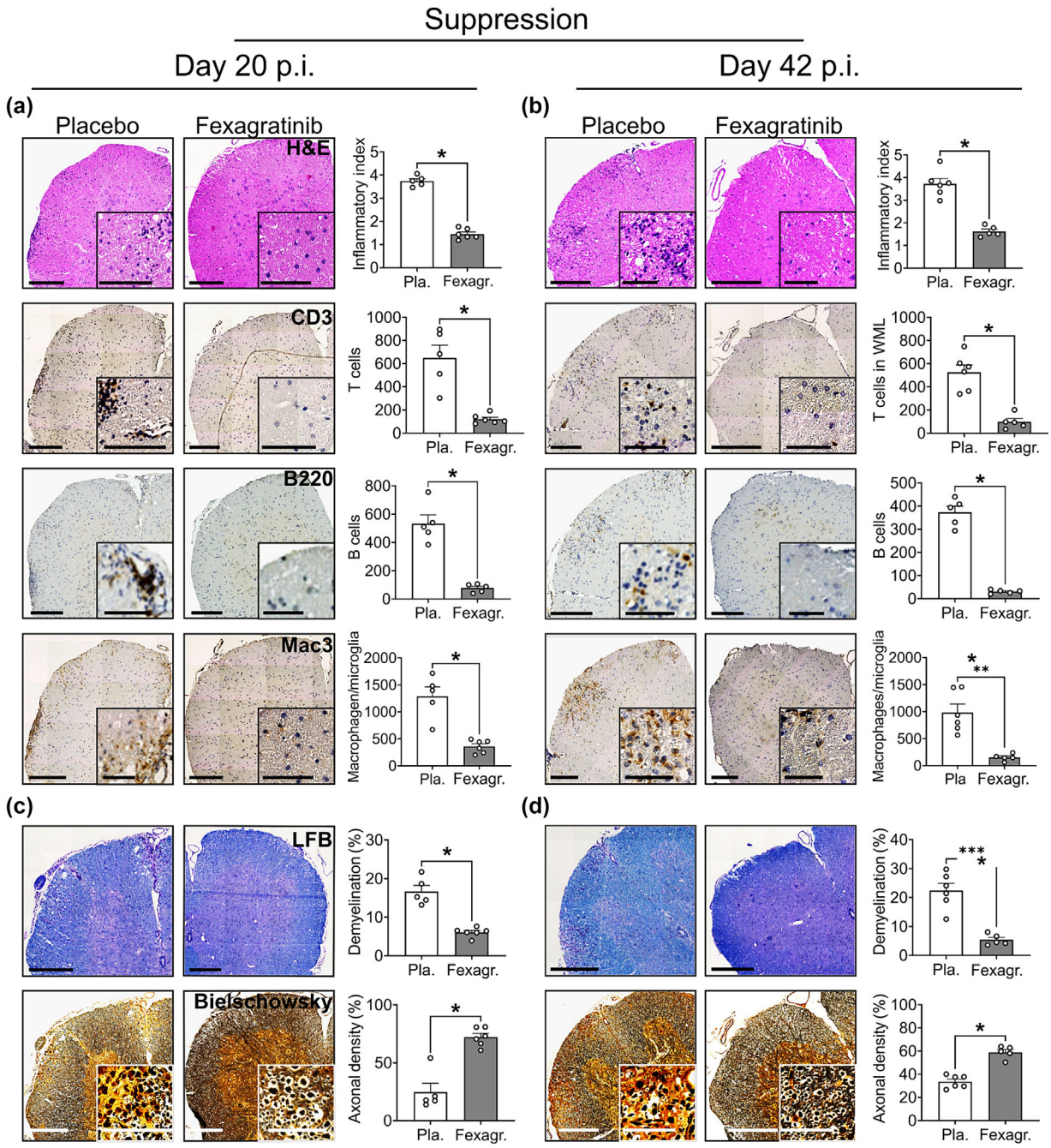

FIGURE 3 Effects of fexagratinib on inflammation and neurodegeneration in the spinal cord (suppression experiment). Inflammatory index, the number of CD3(+) T cells, B220(+) B cells and Mac3(+) macrophages/microglia in white matter lesions (WML) (a) at Day 20 post immunization (p.i.) and (b) at Day 42 p.i. Demyelination (LFB/PAS) and the number of axons (Bielschowsky staining) in WML (c) at Day 20 p.i. and (d) at Day 42 p.i. Representative images of spinal cord sections are shown. Scale bars represent 200 μm and 50 μm. n = 5–6/group. Data are presented as mean ± SEM. Fexagr., fexagratinib; Pla, placebo.

(+) OPCs and p25(+) mature oligodendrocytes in WML was not affected by treatment with fexagratinib (Figure 4c,d). The number of oligodendrocytes in normal appearing white matter (NAWM) remained unchanged by fexagratinib (Figure S1a–d). Application of 12.5 mg of fexagratinib increased CNPase protein expression at Day 18 p.i. (Figure 5d,e). Gene expression levels of remyelination inhibitors were not changed by fexagratinib (Figure S1a,b).

In the suppression experiment, fexagratinib increased the number of Olig2(+) OPCs in WML at Day 20 p.i. (Figure 4e); and a trend towards increased numbers of p25(+) mature oligodendrocytes was observed ($P = 0.1059$) (Figure 4f). At Day 42 p.i., treatment with fexagratinib resulted in an increase in both Olig2(+) OPCs and p25(+) mature oligodendrocytes in WML (Figure 4g,h). In NAWM, the number of Olig2(+) OPCs and p25(+) mature oligodendrocytes was not

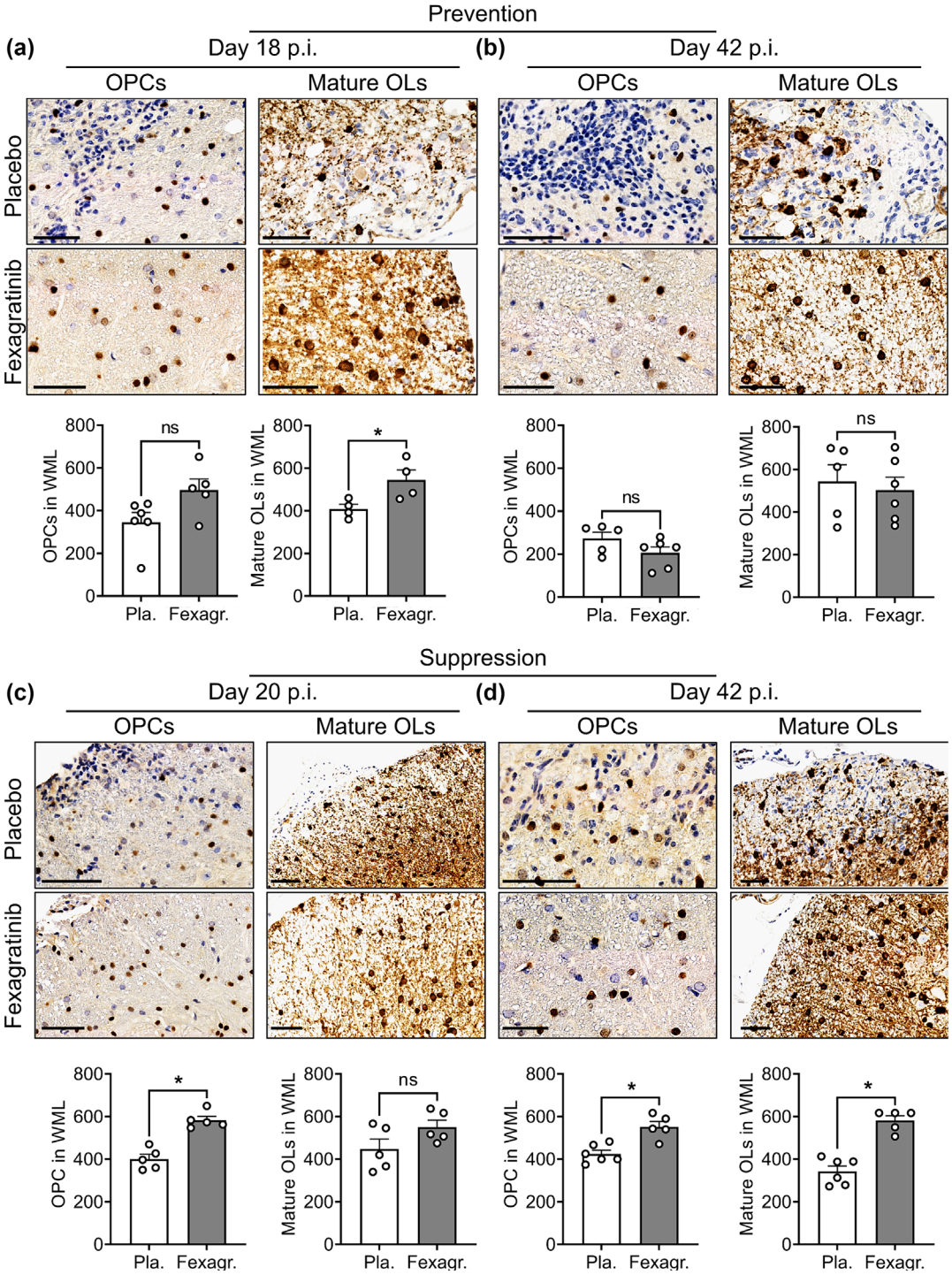

FIGURE 4 Effects of fexagratinib on oligodendrocytes in white matter lesions (WML). (a–d) *Prevention experiment*. (a) oligodendrocyte precursor cells (OPCs) and (b) mature oligodendrocytes (OLs) at Day 18 post immunization (p.i.); (c) OPCs and (d) mature OLs at Day 41 p.i. (e–h) *Suppression experiment*. (e) OPCs and (f) mature OLs at Day 20 p.i.; (g) OPCs and (h) mature OLs at Day 42 p.i. scale bar represents 50 μm. n = 4–7/group. Data are presented as mean ± SEM. Fexagr., fexagratinib; Pla, placebo.

affected by fexagratinib (Figure S1e–h). Administration of 12.5 mg·kg^{-1} of fexagratinib increased expression of myelin proteins at Day 20 p.i. (Figure 6d,e). At Day 42 p.i., no effects of treatment with fexagratinib were observed (Figure 6f,g). Gene expression of remyelination inhibitors was not affected by fexagratinib (Figure S2c,d).

3.4 | The application of fexagratinib alters FGFR, VEGFR-2 and CSFR-dependent pathways as well as TrkB/BDNF expression

Given that fexagratinib inhibits FGFR1-3, VEGFR- 2 and CSFR, we analysed receptor expression and dependent signalling pathways in the spinal cord.

At Day 18 p.i. of the prevention experiment, expression of FGFR1 and FGFR2 remained unchanged by fexagratinib. Application of 12.5 mg·kg^{-1} of fexagratinib resulted in enhanced expression of VEGFR-2 and TrkB, but not CSFR (Figure 5d,e). At Day 41 p.i., 12.5 mg·kg^{-1} of fexagratinib decreased FGFR2. No regulation of VEGFR-2 and CSFR expression was detected at this time point (Figure 5f,g). The downstream proteins ERK, Akt and BDNF of the signalling pathways were not affected by fexagratinib at either time point (Figure 5d–g).

In the suppression experiment, FGFR2 expression was up-regulated by 12.5 mg·kg^{-1} of fexagratinib at Day 20 p.i. BDNF expression was increased after application of 6.25 and 12.5 mg·kg^{-1} of fexagratinib, whereas TrkB was not affected. CSFR was down-regulated at Day 20 p.i. by 12.5 mg·kg^{-1} of fexagratinib, VEGFR-2 was not affected by the treatment (Figure 6d,e). At Day 42 p.i., 12.5 mg·kg^{-1} of fexagratinib increased expression of BDNF, while its receptor TrkB was down-regulated. At this day, 12.5 mg·kg^{-1} of fexagratinib led to an increase in VEGFR-2 expression, while CSFR and FGFR expression remained unchanged (Figure 6f,g).

3.5 | Administration of fexagratinib results in minor regulation of proinflammatory cytokines or chemokines

To assess the effects of fexagratinib on proinflammatory cytokines and chemokines, namely IL-1β, IL-6, IL-12, iNOS, IFN-γ, CX_3CR1 and its ligand CX_3CL1, mRNA analyses were performed using spinal cord tissue through RT-PCR.

In the prevention experiment, mRNA levels of CX_3CL1 were decreased by both 6.25 and 12.5 mg·kg^{-1} of fexagratinib at Day 18 p.i. (Figure S2a). IFN-γ was up-regulated by the 12.5 mg·kg^{-1} dosage at Day 18 p.i., while no changes were observed at Day 41 p.i. (Figure S2a,b).

In the suppression experiment, no changes were found after fexagratinib administration (Figure S2c,d).

3.6 | Application of fexagratinib results in minor regulation of the proportion of peripheral immune cells

To study the effects of fexagratinib on peripheral immune cells, we analysed leukocyte populations, including CD45(+) leukocytes, CD19(+) B cells, CD3(+) T cells, CD8(+) T cells, CD4(+) T cells, CD11b(+) macrophages, CD11c(+) dendritic cells and GR1(+) granulocytes, by flow cytometry in the spleen and blood.

In the prevention experiment, 6.25 mg·kg^{-1} of fexagratinib increased CD45(+) leukocytes in the spleen at Day 18 p.i. (Figure S3a). In the blood, 6.25 mg·kg^{-1} of fexagratinib decreased GR1(+) granulocytes at Day 18 p.i. (Figure S3b). No changes were found in the proportion of other lymphocytes in these tissues. No effects of fexagratinib were observed at Day 41 p.i. (Figures 7a–d and S3a–d).

In the suppression experiment, CD19(+) B cells were decreased by 6.25 mg·kg^{-1} of fexagratinib in the blood at day 20 p.i. (Figure 8b). T cells were not changed at Days 20 p.i. or at Day 42 p.i. A trend towards a down-regulation of CD11b(+) macrophages by 12.5 mg·kg^{-1} was observed in the spleen at Day 20 p.i. (Figure S3e). Fexagratinib did not exert effects on peripheral immune cells in the blood at Days 20 p.i. or 42 p.i. (Figures 8a–d and S3e–h).

3.7 | Fexagratinib application leads to alterations of mitochondrial protein expression

To characterize the effects of fexagratinib on mitochondria, protein expression of SOD2, ATP6E and the ATP synthase β subunit in the spinal cord were measured.

In the prevention experiment, SOD2 expression was increased by 12.5 mg·kg^{-1} of fexagratinib at Day 18 p.i. (Figure 5d,e). At Day 41 p.i., there was a trend towards an up-regulation of SOD2 expression by 12.5 mg·kg^{-1} of fexagratinib (Figure 5f,g).

In the suppression experiment, ATP6E and SOD2 expression (Figure 6d,e) were decreased by both doses of fexagratinib at Day 20 p.i. At Day 42 p.i., 12.5 mg·kg^{-1} of fexagratinib increased SOD2 expression; ATP6E and **ATP synthase β** expression remained unaltered (Figure 5f,g).

4 | DISCUSSION

The effects of the multi-kinase inhibitor fexagratinib in MOG_{35-55}-induced EAE were studied with two experimental approaches. When fexagratinib was given in a dose of 12.5 mg·kg^{-1} in the *prevention experiment*, severe symptoms did not occur (EAE scores ≥ 2.5). In the *suppression experiment*, treatment with 12.5 mg·kg^{-1} of fexagratinib suppressed severe first clinical episodes. In both experiments, effects of 6.25 mg·kg^{-1} of fexagratinib were less pronounced, suggesting a dose–response relationship. When given at a dose of 12.5 mg·kg^{-1}, fexagratinib appears to reduce severe symptoms more efficiently (0%

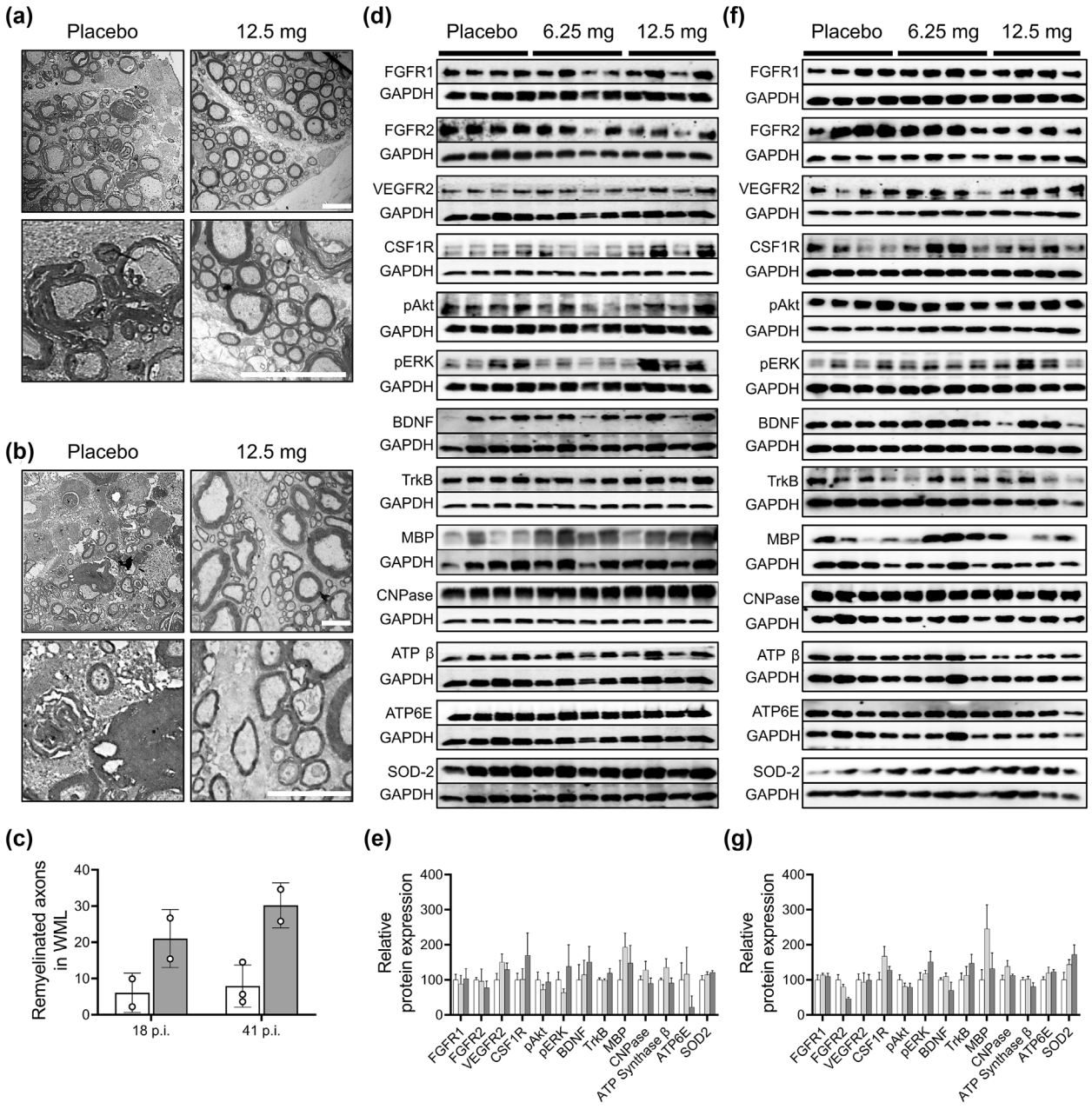

FIGURE 5 Effects of fexagratinib on myelination, signalling pathways, myelin protein expression and mitochondria (prevention experiment). Ultrastructural analysis of white matter lesions (WML) (a) at Days 18 and (b) 41 post immunization (p.i.) (c) Number of remyelinated axons in 2000 μm^2. Scale bar represents 10 μm. Protein expression of FGF-2, FGF-9, FGFR1, FGFR2, VEGFR-2, CSFR, pAkt, pERK, BDNF, TrkB, MBP, CNPase, ATP Synthase Subunit β, ATP6E and SOD2 (d, e) at Day 18 post immunization (p.i.) (n = 4/group) and (f, g) at Day 41 p.i. (n = 4/group). Representative images of spinal cord sections and Western blot images are shown. Data are presented as mean ± SEM.

for fexagratinib vs. 14.3% for infigratinib; acute phase of the prevention experiment). Further, 5.3% of mice treated with infigratinib were affected by severe symptoms at the end of the suppression experiment, whereas 0% of mice treated with fexagratinib showed severe symptoms at this time point.

Reduction of inflammation in the CNS is an important therapeutic goal. In both experiments, application of 12.5 mg·kg^{-1} of fexagratinib decreased lymphocytes and macrophages/microglia in WML at the peak of disease and in the chronic phase of EAE. Immune cells play a key role in the pathophysiology of MS and EAE. In relapses, immune cells migrate across the BBB into the CNS where they cause damage to oligodendrocytes, myelin and axons (Constantinescu et al., 2011). Second, chronic inflammation is known to contribute to ongoing neurodegeneration by the production of reactive oxygen species (ROS) and subsequent mitochondrial dysfunction (Dendrou et al., 2015). The findings on the effects of fexagratinib in EAE suggest that fexagratinib modulates both acute and chronic inflammation. The findings on the reduction of lymphocytes and microglia/macrophages in WML are in

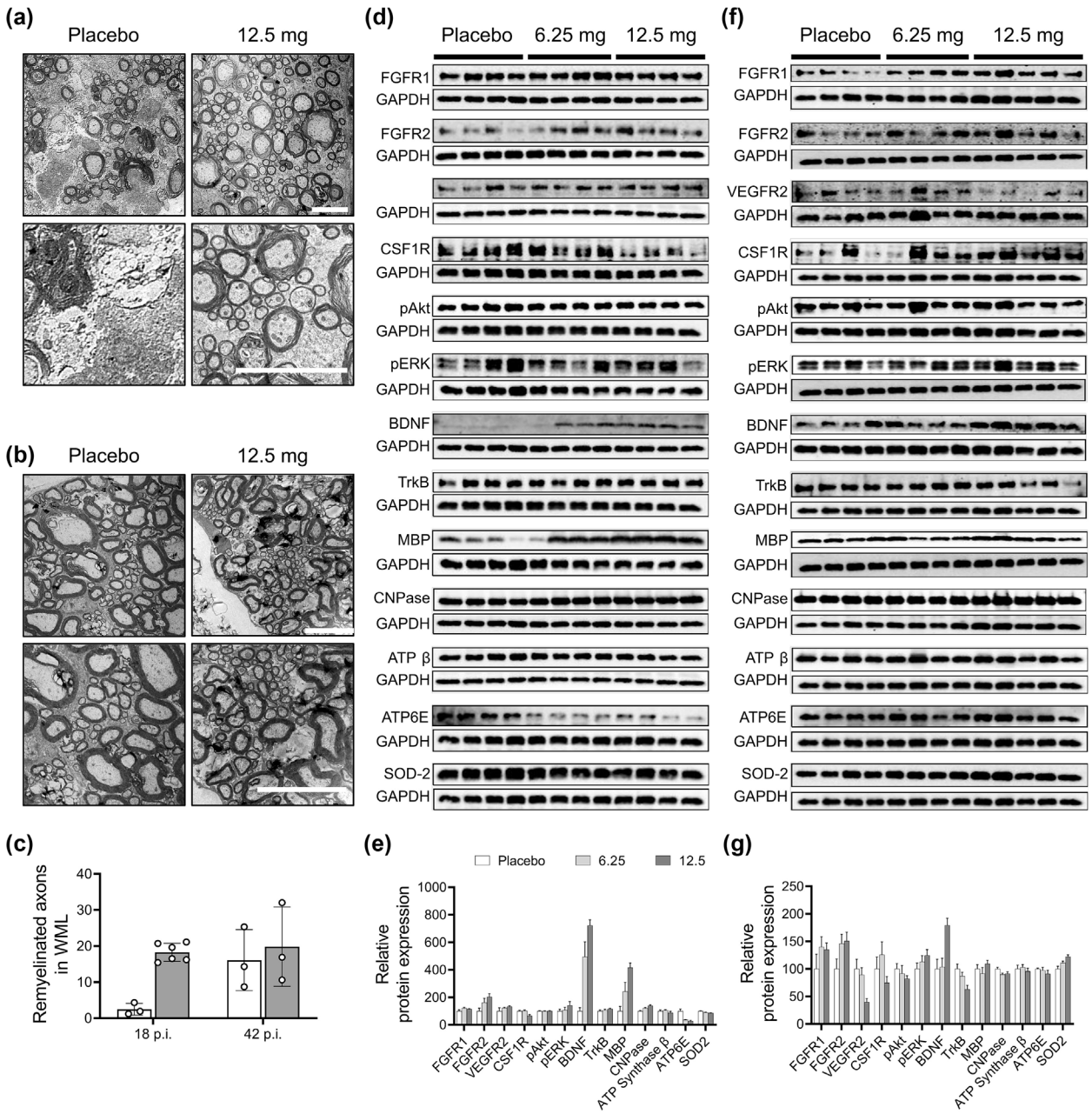

FIGURE 6 Effects of fexagratinib on myelination, signalling pathways, myelin protein expression and mitochondria (suppression experiment). Ultrastructural analysis of white matter lesions (WML) (a) at Days 20 and (b) 42 post immunization (p.i.) (c) Number of remyelinated axons in 2000 μm^2. Scale bar represents 10 μm. Protein expression of FGF-2, FGF-9, FGFR1, FGFR2, VEGFR-2, CSFR, pAkt, pERK, BDNF, TrkB, MBP, CNPase, ATP Synthase Subunit β, ATP6E and SOD2 (d, e) at Day 20 p.i. (n = 4/group) and (f, g) at Day 42 p.i. (n = 4–5/group). Representative images of spinal cord sections and Western blot images are shown. Data are presented as mean ± SEM.

accordance with those from a recent study applying the selective FGFR inhibitor infigratinib (Rajendran et al., 2023).

Effects on the expression of cytokines and chemokines in the CNS were different between the treatment studies. Application of 12.5 mg·kg^{-1} of fexagratinib up-regulated IFNγ, and both 6.25 and 12.5 mg·kg^{-1} of fexagratinib down-regulated CX_3CL1 in the prevention experiment. IFNγ, which is expressed by T cells, macrophages and natural killer cells, activates microglia/macrophages and astrocytes in EAE. CX_3CL1 is expressed by microglia/macrophages and modulates proinflammatory cell–cell interactions in EAE (Limatola & Ransohoff, 2014). CX_3CL1/R1 signalling increases the permeability of the BBB, enhances lymphocytic infiltration in the CNS and accelerates neurodegenerative processes in EAE (Blauth et al., 2015; Iemmolo et al., 2023). Experimental inhibition of the CSFR led to a suppression of cytokines like IL-1β or IL-6 (Hagan et al., 2020), and a reduced number of antigen-presenting-cells

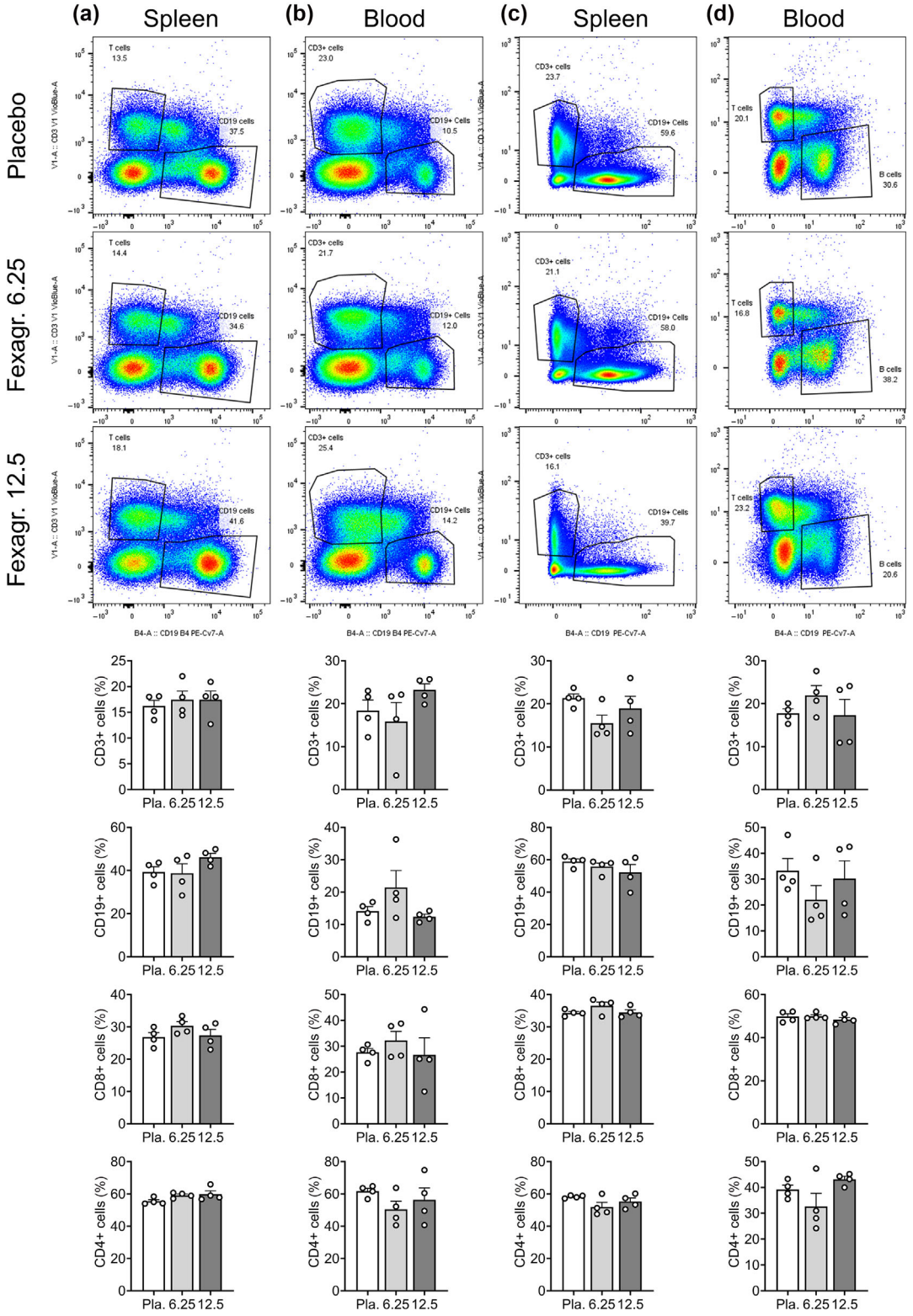

FIGURE 7 Effects of fexagratinib on peripheral immune cells (prevention experiment). FACS analysis of (a) spleen tissue and (b) blood at Day 18 post immunization (p.i.) (n = 4/group). FACS analysis of (c) spleen tissue and (d) blood at Day 41 p.i. (n = 4/group). Data are presented as mean ± SEM. Fexagr., fexagratinib; Pla, placebo.

(Hwang et al., 2022), both which are associated by decreased inflammation in the spinal cord in EAE. VEGFR-2 overexpression results in breakdown of the BBB and enhanced inflammation (Rigau et al., 2007). VEGF also influences the expression of cytokines such as IL-10 or IFNγ (Mor et al., 2004). Inhibition of the VEGFR-2 by SU5416 resulted in an ameliorated disease course (Roscoe et al., 2009).

Remyelination of lesions in MS is impaired (Franklin & Ffrench-Constant, 2017); migration of OPCs to lesions is insufficient, and differentiated oligodendrocytes are found less frequently in chronic lesions (Kuhlmann et al., 2008). In general, intact myelination is required for rapid transmission of action potentials, and the metabolic support of axons. Therefore, degeneration of myelin and the failure of remyelination may lead to a breakdown of cell homeostasis, which may induce and enhance neurodegeneration by energy deficiency and disturbed axonal transport (Franklin & Ffrench-Constant, 2017). Application of 12.5 $mg{\cdot}kg^{-1}$ of fexagratinib resulted in less demyelination and increased axonal density in WML, indicating that multi-kinase inhibition results in neuroprotective effects in EAE. The current findings are in agreement with effects of infigratinib on demyelination and axonal density in both the prevention and suppression experiment. Further, analysis by electron microscopy indicates enhanced remyelination by fexagratinib in both the prevention and suppression experiments, whereas infigratinib induced remyelination just in the suppression experiment (Rajendran et al., 2023). In the chronic phase of the prevention experiment, no effects on the number of OPCs or mature oligodendrocytes were found. In the chronic phase of the suppression experiment, treatment with fexagratinib resulted in an increased number of OPCs and mature oligodendrocytes in lesion areas, a prerequisite for remyelination. These findings suggest that fexagratinib promotes both recruitment and maturation of oligodendrocytes. This is further supported by an in vitro study on the effects of fexagratinib on oligodendrocytes, in which it suppressed expression of FGFR1 and downstream proteins, and enhanced expression BDNF and TrkB, eventually leading to enhanced myelination (Rajendran et al., 2021). The differences between the experimental approaches could depend on the inflammatory milieu, and pharmacological aspects such as the time point of administration and a half-time of 30 h. In focal demyelination models, recruitment of OPCs occurred within the first 10 days p.i., and remyelination took place from Days 10 to 21 p.i., with a maximum at Day 21 p.i. (Franklin & Hinks, 1999). Other studies using models of axonal transection found that initiation of migration and proliferation of OPCs generally takes place within 1 to 7 days after injury, with a maximum after 14 days (Tripathi & McTigue, 2007). We speculate that the suppressive administration of fexagratinib may coincide with the critical timepoint of initiation of migration and proliferation of OPCs, therefore reinforcing the presence of OPCs and mature oligodendrocytes. A relation between VEGFR-2/CSFR and oligodendrocytes was suggested in in other EAE studies. Increased VEGFR-2 levels were measured in demyelinated areas (Sentilhes et al., 2011), and in studies on pharmacological CSFR inhibition, an increased number of oligodendrocytes and reduced demyelination were observed (Marzan et al., 2021).

These findings are in agreement with the recent treatment study, in which the selective FGFR inhibitor infigratinib led to an increase of the number of mature oligodendrocytes (Rajendran et al., 2023).

Decreased expression of *CSFR* by 12.5 $mg{\cdot}kg^{-1}$ of fexagratinib at the peak of the disease was observed in the suppression experiment. Inhibition of the CSFR by the small molecule sotuletinib reduced symptoms of EAE, inflammation and demyelination (Hwang et al., 2022). Another study underlined beneficial effects of pharmacological CSFR inhibition such as suppressed inflammatory cytokines and reduced microglia proliferation (Hagan et al., 2020). Application of 12.5 $mg{\cdot}kg^{-1}$ of fexagratinib decreased expression of *VEGFR2* at the peak of the disease in the prevention experiment. In MS and EAE, VEGF contributes to the degradation of the vascular basement membrane, breakdown of the blood–brain-barrier, and an increase of blood vessel density in lesion areas (Roscoe et al., 2009; Seabrook et al., 2010). In EAE, increased VEGF expression is associated with demyelinated lesions, contributing to the proliferation of OPCs, and down-regulation of inflammatory cytokines and chemokines in microglia/macrophages (Girolamo et al., 2014; Hiratsuka et al., 2019). There is evidence that VEGFR-2 inhibitors reduce symptoms of EAE and decrease inflammation by preventing breakdown of the BBB (Roscoe et al., 2009; Wautier & Wautier, 2022).

Treatment with 12.5 $mg{\cdot}kg^{-1}$ of fexagratinib increased protein expression of **BDNF** in the suppression experiment. BDNF, a member of the neurotrophin family, is expressed by reactive astrocytes, lymphocytes and monocytes (Kerschensteiner et al., 1999; Nociti & Romozzi, 2023). BDNF binds to TrkB, a receptor tyrosine kinase expressed by most neurons in the CNS. BDNF provides differentiation and survival of neurons, neuronal morphogenesis and synaptic plasticity by activation of ERK, Akt, **PLC**/**PKC** and NFκB pathways (Ateaque et al., 2023; Sandhya et al., 2013). The expression of TrkB was up-regulated in the early phase of the disease, but down-regulated in the chronic phase, suggesting that receptor down-regulation is initiated by excessive early supply of BDNF. BDNF also promotes survival and migration of OPCs to lesions (Arai & Lo, 2009). Although up-regulated in active MS lesions, expression in chronic MS plaques is low, which may be one reason for the axonal degeneration in chronic stages of MS (Nociti, 2020). Since administration of fexagratinib up-regulated BDNF expression both at the peak of the disease and in the chronic phase, this increase may have influenced the elevated number of OPCs and oligodendrocytes in WML. Our results are in agreement with pharmacological inhibition of the FGFR by infigratinib, which also resulted in elevated BDNF levels (Rajendran et al., 2023). Taken together, these data provide evidence that treatment with fexagratinib stimulates the secretion of BDNF, thereby decreasing neurodegeneration and severity of symptoms.

In this EAE study, ATP6E was down-regulated after applying fexagratinib at Day 20 p.i. in the suppression experiment. Increased expression of superoxide dismutase (SOD2) was found at Day 18 p.i. of the preventive experiment and Day 42 p.i. of the suppression experiment, and a down-regulation was observed at Day 20 p.i. of the suppression experiment. Mitochondrial dysfunction contributes to neurodegeneration in MS (Witte et al., 2014). ATP6E is a subunit of

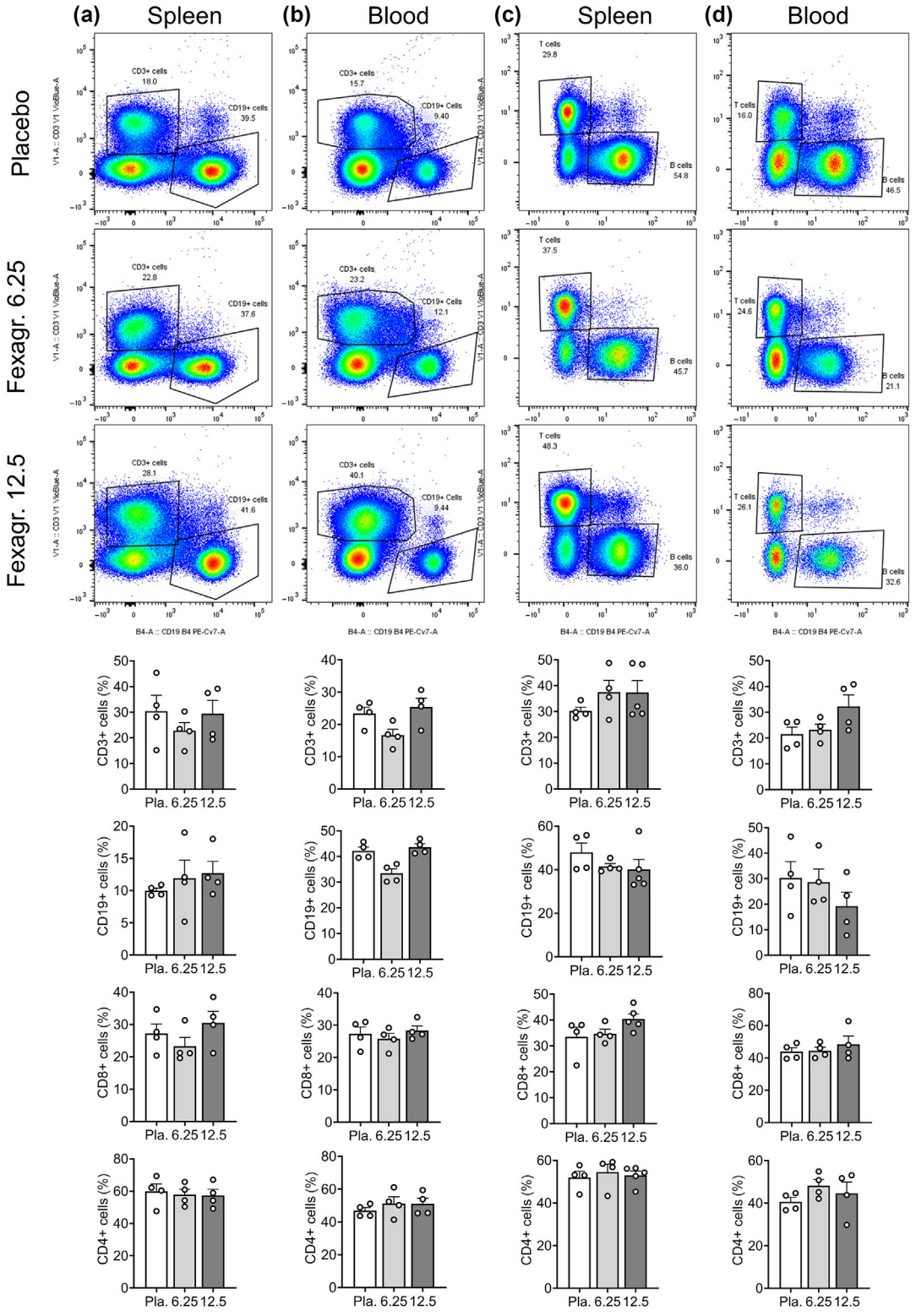

FIGURE 8 Effects of fexagratinib on peripheral immune cells (suppression experiment). FACS analysis of (a) spleen tissue and (b) blood at Day 20 post immunization (p.i.) (n = 4/group). FACS analysis of (c) spleen tissue and (d) blood at Day 42 p.i. (n = 4–5/group). Data are presented as mean ± SEM. Fexagr., fexagratinib; Pla, placebo.

the vacuolar proton ATPase (V-ATPase) (Vanhille et al., 1993), a proton pump important for maintaining the acidity of intracellular compartments such as granules, lysosomes and endosomes (Forgac, 2007). SOD2 is an enzyme located within the mitochondrial matrix that catalyses the reaction of superoxide ($O_2^{\cdot -}$) to hydrogen peroxide (H_2O_2), thereby protecting DNA, proteins and lipids from oxidation.

Furthermore, total functional loss of SOD2 in a *Sod2*$^{-/-}$ deficient mouse model leads to an extensive neurodegeneration due to impaired oxidative metabolism (Flynn & Melovn, 2013). A recently developed *Sod2*$^{-/-}$ model resembles EAE in terms of demyelination and enhanced inflammatory activity, indicating that deficiency of SOD2 is not restricted to neurodegeneration (Bhaskaran et al., 2023). Since reduced neurodegeneration by fexagratinib was observed in the present experiment, effects on mitochondria could have contributed to the preservation of axons by the reduction of oxidative stress.

There are currently 13 clinical trials, including phase I and II trials, registered at the National Library of Medicine in which fexagratinib has been or is currently being tested; most are in patients with tumours. In a phase I trial in patients with solid tumours, fexagratinib showed adverse effects such as gastrointestinal problems, dry mouth and skin and hyperphosphataemia, which were mild to moderate and reversible upon withdrawal of the substance. No dose-limiting toxicities were observed in a Phase Ib study in humans up to a maximum of 160 mg daily (Saka et al., 2017). The equivalent dose of 12.5 mg·kg^{-1} in mice would be 1 mg·kg^{-1} in patients (Nair & Jacob, 2016).

Taken together, oral application of the multi-kinase inhibitor fexagratinib in doses of 6.25 and 12.5 mg·kg^{-1} over 10 days prevented and suppressed first clinical episodes and ameliorated the disease course in a dose dependent manner to the end of the experiment. In the CNS, 12.5 mg·kg^{-1} of fexagratinib decreased infiltration of immune cells in WML, reduced demyelination, and neurodegeneration. Moreover, 12.5 mg·kg^{-1} of fexagratinib increased the number of OPCs and mature oligodendrocytes as well as axonal density in WML and promotes remyelination. Since the substance targets three receptors involved in pathology of EAE, multi-kinase inhibition by fexagratinib in a well-tolerated dose of 1 mg·kg^{-1} in humans may be a promising approach to reduce inflammation and neurodegeneration, to slow down disease progression and support remyelination in patients. Synergetic inhibition of pathways by fexagratinib may lead to a stronger reduction of symptoms and demyelination, and enhanced axonal preservation than selective FGFR inhibition.

AUTHOR CONTRIBUTIONS

Martin Berghoff and Ranjithkumar Rajendran did the conceptualization. Fynn Gurski, Kian Shirvanchi, Vinothkumar Rajendran, Ranjithkumar Rajendran and Sudhanshu Bhushan performed experiments. Fynn Gurski, Kian Shirvanchi, Fevronia-Foivi Megalofonou and Martin Berghoff analysed the data. Martin Berghoff, Srikanth Karnati, and Christine Stadelmann supervised the experiments. Fynn Gurski, Kian Shirvanchi, Gregor Böttiger and Martin Berghoff wrote the original draft of manuscript. All authors reviewed and edited the final manuscript.

ACKNOWLEDGEMENTS

Open Access funding enabled and organized by Projekt DEAL.

CONFLICT OF INTEREST STATEMENT

The authors report no competing interests.

DATA AVAILABILITY STATEMENT

The data that support the findings of this study are available from the corresponding author upon reasonable request. Some data may not be made available because of privacy or ethical restrictions.

DECLARATION OF TRANSPARENCY AND SCIENTIFIC RIGOUR

This Declaration acknowledges that this paper adheres to the principles for transparent reporting and scientific rigour of preclinical research as stated in the BJP guidelines for Natural Products Research, Design and Analysis, Immunoblotting and Immunochemistry, and Animal Experimentation, and as recommended by funding agencies, publishers and other organisations engaged with supporting research.

ORCID

Kian Shirvanchi https://orcid.org/0000-0002-8297-3855
Vinothkumar Rajendran https://orcid.org/0000-0001-9425-8579

REFERENCES

Alexander, S. P. H., Christopoulos, A., Davenport, A. P., Kelly, E., Mathie, A. A., Peters, J. A., Veale, E. L., Armstrong, J. F., Faccenda, E., Harding, S. D., Davies, J. A., Abbracchio, M. P., Abraham, G., Agoulnik, A., Alexander, W., Al-Hosaini, K., Bäck, M., Baker, J. G., Barnes, N. M., … Ye, R. D. (2023). The Concise Guide to PHARMACOLOGY 2023/24: G protein-coupled receptors. *British Journal of Pharmacology*, *180*, S23–S144. https://doi.org/10.1111/bph.16177

Alexander, S. P. H., Fabbro, D., Kelly, E., Mathie, A. A., Peters, J. A., Veale, E. L., Armstrong, J. F., Faccenda, E., Harding, S. D., Davies, J. A., Amarosi, L., Anderson, C. M. H., Beart, P. M., Broer, S., Dawson, P. A., Gyimesi, G., Hagenbuch, B., Hammond, J. R., Hancox, J. C., … Verri, T. (2023). The Concise Guide to PHARMACOLOGY 2023/24: Transporters. *British Journal of Pharmacology*, *180*, S374–S469. https://doi.org/10.1111/bph.16182

Alexander, S. P. H., Fabbro, D., Kelly, E., Mathie, A. A., Peters, J. A., Veale, E. L., Armstrong, J. F., Faccenda, E., Harding, S. D., Davies, J. A., Annett, S., Boison, D., Burns, K. E., Dessauer, C., Gertsch, J., Helsby, N. A., Izzo, A. A., Ostrom, R., Papapetropoulos, A., … Wong, S. S. (2023). The Concise Guide to PHARMACOLOGY 2023/24: Enzymes. *British Journal of Pharmacology*, *180*, S289–S373. https://doi.org/10.1111/bph.16181

Alexander, S. P. H., Fabbro, D., Kelly, E., Mathie, A. A., Peters, J. A., Veale, E. L., Armstrong, J. F., Faccenda, E., Harding, S. D., Davies, J. A., Beuve, A., Brouckaert, P., Bryant, C., Burnett, J. C., Farndale, R. W., Friebe, A., Garthwaite, J., Hobbs, A. J., Jarvis, G. E., … Waldman, S. A. (2023). The Concise Guide to PHARMACOLOGY 2023/24: Catalytic receptors. *British Journal of Pharmacology*, *180*, S241–S288. https://doi.org/10.1111/bph.16180

Alexander, S. P. H., Roberts, R. E., Broughton, B. R. S., Sobey, C. G., George, C. H., Stanford, S. C., Cirino, G., Docherty, J. R., Giembycz, M. A., Hoyer, D., Insel, P. A., Izzo, A. A., Ji, Y., MacEwan, D. J., Mangum, J., Wonnacott, S., & Ahluwalia, A. (2018). Goals and practicalities of immunoblotting and immunohistochemistry: A guide for submission to the *British Journal of Pharmacology*. *British Journal of Pharmacology*, *175*, 407–411. https://doi.org/10.1111/bph.14112

Amini Harandi, A., Siavoshi, F., Shirzadeh Barough, S., Amini Harandi, A., Pakdaman, H., Sahraian, M. A., Fathtabar, Z., Mohammadi, F., Karamiani, F., & Ardehali, S. H. (2022). Vascular endothelial growth factor as a predictive and prognostic biomarker for multiple sclerosis. *Neuroimmunomodulation*, *29*(4), 476–485. https://doi.org/10.1159/000525600

Arai, K., & Lo, E. H. (2009). An oligovascular niche: Cerebral endothelial cells promote the survival and proliferation of oligodendrocyte precursor cells. *The Journal of Neuroscience: the Official Journal of the Society for Neuroscience*, *29*(14), 4351–4355. https://doi.org/10.1523/JNEUROSCI.0035-09.2009

Ateaque, S., Merkouris, S., & Barde, Y.-A. (2023). Neurotrophin signalling in the human nervous system. *Frontiers in Molecular Neuroscience*, *16*, 1225373. https://doi.org/10.3389/FNMOL.2023.1225373

Bhaskaran, S., Kumar, G., Thadathil, N., Piekarz, K. M., Mohammed, S., Lopez, S. D., Qaisar, R., Walton, D., Brown, J. L., Murphy, A., Smith, N., Saunders, D., Beckstead, M. J., Plafker, S., Lewis, T. L., Towner, R., Deepa, S. S., Richardson, A., Axtell, R. C., & Van Remmen, H. (2023). Neuronal deletion of MnSOD in mice leads to demyelination, inflammation and progressive paralysis that mimics phenotypes associated with progressive multiple sclerosis. *Redox Biology*, *59*, 102550. https://doi.org/10.1016/J.REDOX.2022.102550

Blauth, K., Zhang, X., Chopra, M., Rogan, S., & Markovic-Plese, S. (2015). The role of fractalkine (CX3CL1) in regulation of CD4(+) cell migration to the central nervous system in patients with relapsing-remitting multiple sclerosis. *Clinical Immunology (Orlando, Fla.)*, *157*(2), 121–132. https://doi.org/10.1016/J.CLIM.2015.01.001

Cadavid, D., Mellion, M., Hupperts, R., Edwards, K. R., Calabresi, P. A., Drulović, J., Giovannoni, G., Hartung, H. P., Arnold, D. L., Fisher, E., Rudick, R., Mi, S., Chai, Y., Li, J., Zhang, Y., Cheng, W., Xu, L., Zhu, B., Green, S. M., … Zielinski, T. (2019). Safety and efficacy of opicinumab in patients with relapsing multiple sclerosis (SYNERGY): A randomised, placebo-controlled, phase 2 trial. *The Lancet. Neurology*, *18*(9), 845–856. https://doi.org/10.1016/S1474-4422(19)30137-1

Charabati, M., Wheeler, M. A., Weiner, H. L., & Quintana, F. J. (2023). Multiple sclerosis: Neuroimmune crosstalk and therapeutic targeting. *Cell*, *186*(7), 1309–1327. https://doi.org/10.1016/J.CELL.2023.03.008

Chisari, C. G., Sgarlata, E., Arena, S., Toscano, S., Luca, M., & Patti, F. (2022). Rituximab for the treatment of multiple sclerosis: A review. *Journal of Neurology*, *269*(1), 159–183. https://doi.org/10.1007/S00415-020-10362-Z

Clemente, D., Ortega, M. C., Arenzana, F. J., & de Castro, F. (2011). FGF-2 and anosmin-1 are selectively expressed in different types of multiple sclerosis lesions. *Journal of Neuroscience*, *31*(42), 14899–14909. https://doi.org/10.1523/JNEUROSCI.1158-11.2011

Constantinescu, C. S., Farooqi, N., O'Brien, K., & Gran, B. (2011). Experimental autoimmune encephalomyelitis (EAE) as a model for multiple sclerosis (MS). *British Journal of Pharmacology*, *164*(4), 1079–1106. https://doi.org/10.1111/J.1476-5381.2011.01302.X

Curtis, M. J., Alexander, S. P. H., Cirino, G., George, C. H., Kendall, D. A., Insel, P. A., Izzo, A. A., Ji, Y., Panettieri, R. A., Patel, H. H., Sobey, C. G., Stanford, S. C., Stanley, P., Stefanska, B., Stephens, G. J., Teixeira, M. M., Vergnolle, N., & Ahluwalia, A. (2022). Planning experiments: Updated guidance on experimental design and analysis and their reporting III. *British Journal of Pharmacology*, 179(15), 3907–3913. https://doi.org/10.1111/bph.15868

Dendrou, C. A., Fugger, L., & Friese, M. A. (2015). Immunopathology of multiple sclerosis. *Nature Reviews. Immunology*, *15*(9), 545–558. https://doi.org/10.1038/NRI3871

Derdelinckx, J., Cras, P., Berneman, Z. N., & Cools, N. (2021). Antigen-specific treatment modalities in MS: The past, the present, and the future. *Frontiers in Immunology*, *12*, 624685. https://doi.org/10.3389/FIMMU.2021.624685

Flynn, J. M., & Melovn, S. (2013). SOD2 in mitochondrial dysfunction and neurodegeneration. *Free Radical Biology & Medicine*, *62*, 4–12. https://doi.org/10.1016/J.FREERADBIOMED.2013.05.027

Forgac, M. (2007). Vacuolar ATPases: Rotary proton pumps in physiology and pathophysiology. *Nature Reviews. Molecular Cell Biology*, *8*(11), 917–929. https://doi.org/10.1038/NRM2272

Franklin, R. J. M., & Ffrench-Constant, C. (2017). Regenerating CNS myelin - from mechanisms to experimental medicines. *Nature Reviews. Neuroscience*, *18*(12), 753–769. https://doi.org/10.1038/NRN.2017.136

Franklin, R. J. M., & Hinks, G. L. (1999). Understanding CNS remyelination: Clues from developmental and regeneration biology. *Journal of Neuroscience Research*, *58*(2), 207–213. https://doi.org/10.1002/(SICI)1097-4547(19991015)58:2<207::AID-JNR1>3.0.CO;2-1

Freeman, L., Longbrake, E. E., Coyle, P. K., Hendin, B., & Vollmer, T. (2022). High-efficacy therapies for treatment-Naïve individuals with relapsing–remitting multiple sclerosis. *CNS Drugs*, *36*(12), 1285–1299. https://doi.org/10.1007/S40263-022-00965-7

Gavine, P. R., Mooney, L., Kilgour, E., Thomas, A. P., Al-Kadhimi, K., Beck, S., Rooney, C., Coleman, T., Baker, D., Mellor, M. J., Brooks, A. N., & Klinowska, T. (2012). Fexagratinib: An orally bioavailable, potent, and selective inhibitor of the fibroblast growth factor receptor tyrosine kinase family. *Cancer Research*, *72*(8), 2045–2056. https://doi.org/10.1158/0008-5472.CAN-11-3034

Girolamo, F., Coppola, C., Ribatti, D., & Trojano, M. (2014). Angiogenesis in multiple sclerosis and experimental autoimmune encephalomyelitis. *Acta Neuropathologica Communications*, *2*(1), 84. https://doi.org/10.1186/S40478-014-0084-Z

Hagan, N., Kane, J. L., Grover, D., Woodworth, L., Madore, C., Saleh, J., Sancho, J., Liu, J., Li, Y., Proto, J., Zelic, M., Mahan, A., Kothe, M., Scholte, A. A., Fitzgerald, M., Gisevius, B., Haghikia, A., Butovsky, O., & Ofengeim, D. (2020). CSF1R signaling is a regulator of pathogenesis in progressive MS. *Cell Death and Disease*, *11*(10), 904. https://doi.org/10.1038/s41419-020-03084-7

Hiratsuka, D., Kurganov, E., Furube, E., Morita, M., & Miyata, S. (2019). VEGF- and PDGF-dependent proliferation of oligodendrocyte progenitor cells in the medulla oblongata after LPC-induced focal demyelination. *Journal of Neuroimmunology*, *332*, 176–186. https://doi.org/10.1016/J.JNEUROIM.2019.04.016

Hwang, D., Seyedsadr, M. S., Ishikawa, L. L. W., Boehm, A., Sahin, Z., Casella, G., Jang, S., Gonzalez, M. V., Garifallou, J. P., Hakonarson, H., Zhang, W., Xiao, D., Rostami, A., Zhang, G. X., & Ciric, B. (2022). CSF-1 maintains pathogenic but not homeostatic myeloid cells in the central nervous system during autoimmune neuroinflammation. *Proceedings of the National Academy of Sciences of the United States of America*, *119*(14), e2111804119. https://doi.org/10.1073/PNAS.2111804119/-/DCSUPPLEMENTAL

Iemmolo, M., Ghersi, G., & Bivona, G. (2023). The cytokine CX3CL1 and ADAMs/MMPs in concerted cross-talk influencing neurodegenerative diseases. *International Journal of Molecular Sciences*, *24*(9), 8026. https://doi.org/10.3390/IJMS24098026

Kamali, S., Rajendran, R., Stadelmann, C., Karnati, S., Rajendran, V., Giraldo-Velasquez, M., & Berghoff, M. (2021). Oligodendrocyte-specific deletion of FGFR2 ameliorates MOG35-55-induced EAE through ERK and Akt signalling. *Brain Pathology.*, *31*, 297–311. https://doi.org/10.1111/bpa.12916

Kerschensteiner, M., Gallmeier, E., Behrens, L., Leal, V. V., Misgeld, T., Klinkert, W. E. F., Kolbeck, R., Hoppe, E., Oropeza-Wekerle, R. L., Bartke, I., Stadelmann, C., Lassmann, H., Wekerle, H., & Hohlfeld, R. (1999). Activated human T cells, B cells, and monocytes produce brain-derived neurotrophic factor in vitro and in inflammatory brain lesions: A neuroprotective role of inflammation? *The Journal of Experimental Medicine*, *189*(5), 865–870. https://doi.org/10.1084/JEM.189.5.865

Khoy, K., Mariotte, D., Defer, G., Petit, G., Toutirais, O., & Le Mauff, B. (2020). Natalizumab in multiple sclerosis treatment: From biological effects to immune monitoring. *Frontiers in Immunology*, *11*, 549842. https://doi.org/10.3389/FIMMU.2020.549842

Kuhlmann, T., Lassmann, H., & Brück, W. (2008). Diagnosis of inflammatory demyelination in biopsy specimens: A practical approach. *Acta Neuropathologica*, *115*(3), 275–287. https://doi.org/10.1007/S00401-007-0320-8

Kunkl, M., Frascolla, S., Amormino, C., Volpe, E., & Tuosto, L. (2020). T helper cells: The modulators of inflammation in multiple sclerosis. *Cells*, *9*(2), 482. https://doi.org/10.3390/CELLS9020482

Lassmann, H. (2019). Pathogenic mechanisms associated with different clinical courses of multiple sclerosis. *Frontiers in immunology*, *9*, 3116. https://doi.org/10.3389/fimmu.2018.03116

Lilley, E., Stanford, S. C., Kendall, D. E., Alexander, S. P. H., Cirino, G., Docherty, J. R., George, C. H., Insel, P. A., Izzo, A. A., Ji, Y., Panettieri, R. A., Sobey, C. G., Stefanska, B., Stephens, G., Teixeira, M., & Ahluwalia, A. (2020). ARRIVE 2.0 and the *British Journal of Pharmacology*: Updated guidance for 2020. *British Journal of Pharmacology*, *177*(16), 3611-3616. https://doi.org/10.1111/bph.15178

Limatola, C., & Ransohoff, R. M. (2014). Modulating neurotoxicity through CX3CL1/CX3CR1 signaling. *Frontiers in Cellular Neuroscience*, *8*(AUG), 229. https://doi.org/10.3389/FNCEL.2014.00229

Mahad, D. H., Trapp, B. D., & Lassmann, H. (2015). Pathological mechanisms in progressive multiple sclerosis. In *The lancet neurology* (Vol. 14, Issue 2) (pp. 183–193). Lancet Publishing Group. https://doi.org/10.1016/S1474-4422(14)70256-X

Marzan, D. E., Brügger-Verdon, V., West, B. L., Liddelow, S., Samanta, J., & Salzer, J. L. (2021). Activated microglia drive demyelination via CSF1R signaling. *Glia*, *69*(6), 1583–1604. https://doi.org/10.1002/GLIA.23980

Mohan, H., Friese, A., Albrecht, S., Krumbholz, M., Elliott, C. L., Arthur, A., Menon, R., Farina, C., Junker, A., Stadelmann, C., Barnett, S. C., Huitinga, I., Wekerle, H., Hohlfeld, R., Lassmann, H., Kuhlmann, T., Linington, C., & Meinl, E. (2014). Transcript profiling of different types of multiple sclerosis lesions yields FGF1 as a promoter of remyelination. *Acta Neuropathologica Communications*, *2*(1), 168. https://doi.org/10.1186/s40478-014-0168-9

Mor, F., Quintana, F. J., & Cohen, I. R. (2004). Angiogenesis-inflammation cross-talk: Vascular endothelial growth factor is secreted by activated T cells and induces Th1 polarization. *Journal of Immunology (Baltimore, Md.: 1950)*, *172*(7), 4618–4623. https://doi.org/10.4049/JIMMUNOL.172.7.4618

Nair, A., & Jacob, S. (2016). A simple practice guide for dose conversion between animals and human. *Journal of Basic and Clinical Pharmacy*, *7*(2), 27–31. https://doi.org/10.4103/0976-0105.177703

Nociti, V. (2020). What is the role of brain derived neurotrophic factor in multiple sclerosis neuroinflammation? *Neuroimmunology and Neuroinflammation*, *7*(3), 291–299. https://doi.org/10.20517/2347-8659.2020.25

Nociti, V., & Romozzi, M. (2023). The role of BDNF in multiple sclerosis Neuroinflammation. *International Journal of Molecular Sciences*, *24*(9), 8447. https://doi.org/10.3390/IJMS24098447

Paik, P. K., Shen, R., Berger, M. F., Ferry, D., Soria, J. C., Mathewson, A., Rooney, C., Smith, N. R., Cullberg, M., Kilgour, E., Landers, D., Frewer, P., Brooks, N., & Andre, F. (2017). A phase 1b open label multicentre study of fexagratinib in patients with advanced squamous cell lung cancers. *Clinical Cancer Research: an Official Journal of the American Association for Cancer Research*, *23*(18), 5366–5373. https://doi.org/10.1158/1078-0432.CCR-17-0645

Percie du Sert, N., Hurst, V., Ahluwalia, A., Alam, S., Avey, M. T., Baker, M., Browne, W. J., Clark, A., Cuthill, I. C., Dirnagl, U., Emerson, M., Garner, P., Holgate, S. T., Howells, D. W., Karp, N. A., Lazic, S. E., Lidster, K., MacCallum, C. J., Macleod, M., … Würbel, H. (2020). The ARRIVE guidelines 2.0: Updated guidelines for reporting animal research. *PLoS Biology*, *18*(7), e3000410. https://doi.org/10.1371/journal.pbio.3000410

Proescholdt, M. A., Jacobson, S., Tresser, N., Oldfield, E. H., & Merrill, M. J. (2002). Vascular endothelial growth factor is expressed in multiple sclerosis plaques and can induce inflammatory lesions in experimental allergic encephalomyelitis rats. *Journal of Neuropathology and Experimental Neurology*, *61*(10), 914–925. https://doi.org/10.1093/JNEN/61.10.914

Rajendran, R., Böttiger, G., Dentzien, N., Rajendran, V., Sharifi, B., Ergün, S., Stadelmann, C., Karnati, S., & Berghoff, M. (2021). Effects of FGFR tyrosine kinase inhibition in OLN-93 oligodendrocytes. *Cells*, *10*(6), 1318. https://doi.org/10.3390/cells10061318

Rajendran, R., Rajendran, V., Böttiger, G., Stadelmann, C., Shirvanchi, K., von Au, L., Bhushan, S., Wallendszus, N., Schunin, D., Westbrock, V., Liebisch, G., Ergün, S., Karnati, S., & Berghoff, M. (2023). The small molecule fibroblast growth factor receptor inhibitor infigratinib exerts anti-inflammatory effects and remyelination in a model of multiple sclerosis. *British Journal of Pharmacology*., *180*, 2989–3007. https://doi.org/10.1111/bph.16186

Rajendran, R., Rajendran, V., Giraldo-velasquez, M., Megalofonou, F. F., Gurski, F., Stadelmann, C., Karnati, S., & Berghoff, M. (2021). Oligodendrocyte-specific deletion of fgfr1 reduces cerebellar inflammation and neurodegeneration in mog35-55-induced eae. *International Journal of Molecular Sciences*, *22*(17), 9495. https://doi.org/10.3390/ijms22179495

Reich, D. S., Lucchinetti, C. F., & Calabresi, P. A. (2018). Multiple Sclerosis. *New England Journal of Medicine*, *378*(2), 169–180. https://doi.org/10.1056/NEJMra1401483

Rigau, V., Morin, M., Rousset, M. C., De Bock, F., Lebrun, A., Coubes, P., Picot, M. C., Baldy-Moulinier, M., Bockaert, J., Crespel, A., & Lerner-Natoli, M. (2007). Angiogenesis is associated with blood-brain barrier permeability in temporal lobe epilepsy. *Brain: a Journal of Neurology*, *130*(Pt 7), 1942–1956. https://doi.org/10.1093/BRAIN/AWM118

Roscoe, W. A., Welsh, M. E., Carter, D. E., & Karlik, S. J. (2009). VEGF and angiogenesis in acute and chronic MOG(35-55) peptide induced EAE. *Journal of Neuroimmunology*, *209*(1–2), 6–15. https://doi.org/10.1016/j.jneuroim.2009.01.009

Roy, R., Alotaibi, A. A., & Freedman, M. S. (2021). Sphingosine 1-phosphate receptor modulators for multiple sclerosis. *CNS Drugs*, *35*(4), 385–402. https://doi.org/10.1007/S40263-021-00798-W

Saka, H., Kitagawa, C., Kogure, Y., Takahashi, Y., Fujikawa, K., Sagawa, T., Iwasa, S., Takahashi, N., Fukao, T., Tchinou, C., Landers, D., & Yamada, Y. (2017). Safety, tolerability and pharmacokinetics of the fibroblast growth factor receptor inhibitor fexagratinib in Japanese patients with advanced solid tumours: A phase I study. *Investigational New Drugs*, *35*(4), 451–462. https://doi.org/10.1007/S10637-016-0416-X

Sandhya, V. K., Raju, R., Verma, R., Advani, J., Sharma, R., Radhakrishnan, A., Nanjappa, V., Narayana, J., Somani, B. L., Mukherjee, K. K., Pandey, A., Christopher, R., & Keshava Prasad, T. S. (2013). A network map of BDNF/TRKB and BDNF/p75NTR signaling system. *Journal of Cell Communication and Signaling*, *7*(4), 301–307. https://doi.org/10.1007/S12079-013-0200-Z

Sarchielli, P., Di Filippo, M., Ercolani, M. V., Chiasserini, D., Mattioni, A., Bonucci, M., Tenaglia, S., Eusebi, P., & Calabresi, P. (2008). Fibroblast growth factor-2 levels are elevated in the cerebrospinal fluid of multiple sclerosis patients. *Neuroscience Letters*, *435*(3), 223–228. https://doi.org/10.1016/J.NEULET.2008.02.040

Seabrook, T. J., Littlewood-Evans, A., Brinkmann, V., Pöllinger, B., Schnell, C., & Hiestand, P. C. (2010). Angiogenesis is present in experimental autoimmune encephalomyelitis and pro-angiogenic factors are increased in multiple sclerosis lesions. *Journal of Neuroinflammation*, *7*, 95. https://doi.org/10.1186/1742-2094-7-95

Sentilhes, L., Marret, S., Leroux, P., Gonzalez, B. J., & Laquerrière, A. (2011). Vascular-endothelial growth factor and its high affinity receptor VEGFR-2 in the normal versus destructive lesions human forebrain during development: An immuno-histochemical comparative study. *Brain Research*, *1385*, 77–86. https://doi.org/10.1016/j.brainres.2011.01.111

Su, J. J., Osoegawa, M., Matsuoka, T., Minohara, M., Tanaka, M., Ishizu, T., Mihara, F., Taniwaki, T., & Kira, J. I. (2006). Upregulation of vascular growth factors in multiple sclerosis: Correlation with MRI findings. *Journal of the Neurological Sciences*, *243*(1–2), 21–30. https://doi.org/10.1016/j.jns.2005.11.006

Tripathi, R., & McTigue, D. M. (2007). Prominent oligodendrocyte genesis along the border of spinal contusion lesions. *Glia*, *55*(7), 698–711. https://doi.org/10.1002/GLIA.20491

Vanhille, B., Vanek, M., Richener, H., Green, J. R., & Bilbe, G. (1993). Cloning and tissue distribution of subunit C, D and E of the human vacuolar H+-ATPase. *Biochemical and Biophysical Research Communications*, *197*(1), 15–21. https://doi.org/10.1006/bbrc.1993.2434

Walton, C., King, R., Rechtman, L., Kaye, W., Leray, E., Marrie, R. A., Robertson, N., La Rocca, N., Uitdehaag, B., van der Mei, I., Wallin, M., Helme, A., Angood Napier, C., Rijke, N., & Baneke, P. (2020). Rising prevalence of multiple sclerosis worldwide: Insights from the atlas of MS, third edition. *Multiple Sclerosis Journal*, *26*(14), 1816–1821. https://doi.org/10.1177/1352458520970841

Wautier, J. L., & Wautier, M. P. (2022). Vascular permeability in diseases. In *International journal of molecular sciences*, *23*(7), 3645. https://doi.org/10.3390/ijms23073645

Witte, M. E., Mahad, D. J., Lassmann, H., & van Horssen, J. (2014). Mitochondrial dysfunction contributes to neurodegeneration in multiple sclerosis. *Trends in Molecular Medicine*, *20*(3), 179–187. https://doi.org/10.1016/J.MOLMED.2013.11.007

SUPPORTING INFORMATION

Additional supporting information can be found online in the Supporting Information section at the end of this article.

How to cite this article: Gurski, F., Shirvanchi, K., Rajendran, V., Rajendran, R., Megalofonou, F.-F., Böttiger, G., Stadelmann, C., Bhushan, S., Ergün, S., Karnati, S., & Berghoff, M. (2025). Anti-inflammatory and remyelinating effects of fexagratinib in experimental multiple sclerosis. *British Journal of Pharmacology*, *182*(1), 142–161. https://doi.org/10.1111/bph.17341